



MASTER THESIS

---

# Remote Monitoring of Animals Vital Functions by Using IoT

---

*Author:*  
Bc. Markéta BULÍNOVÁ

*Supervisor:*  
Doc. Ing. Jiří MASOPUST, CSc.

*A thesis submitted in fulfillment of the requirements  
for the degree of Engineer (Ing.)*

*in the*

Faculty of Electrical Engineering

Department of Applied Electronics and Telecommunications

May 26, 2019

ZÁPADOČESKÁ UNIVERZITA V PLZNI  
Fakulta elektrotechnická  
Akademický rok: 2018/2019

**ZADÁNÍ DIPLOMOVÉ PRÁCE**  
(PROJEKTU, UMĚLECKÉHO DÍLA, UMĚLECKÉHO VÝKONU)

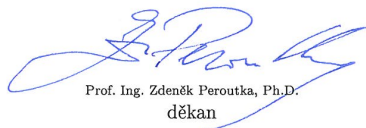
Jméno a příjmení: **Bc. Markéta BULÍNOVÁ**  
Osobní číslo: **E16N0065P**  
Studijní program: **N2612 Elektrotechnika a informatika**  
Studijní obor: **Telekomunikační a multimediální systémy**  
Název tématu: **Dálkový monitoring životních funkcí domácích zvířat  
s využitím IoT**  
Zadávající katedra: **Katedra aplikované elektroniky a telekomunikací**

Z á s a d y p r o v y p r a c o v á n í :

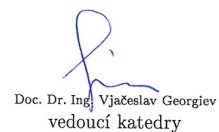
1. Prostudujte a popište možnosti monitoringu životních funkcí domácích zvířat.
2. Prostudujte a popište možnosti dálkového přenosu dat z nositelné elektroniky.
3. Navrhněte systém monitoringu životních funkcí, přenosu získaných dat a jejich vyhodnocení u vybraného domácího zvířete včetně vizualizace.
4. Dle možností navržený systém realizujte.

Rozsah grafických prací: podle doporučení vedoucího  
Rozsah kvalifikační práce: 40 - 60 stran  
Forma zpracování diplomové práce: tištěná/elektronická  
Seznam odborné literatury:  
<https://iot.plzen.eu/>

Vedoucí diplomové práce: **Doc. Ing. Jiří Masopust, CSc.**  
Katedra aplikované elektroniky a telekomunikací  
Datum zadání diplomové práce: **5. října 2018**  
Termín odevzdání diplomové práce: **30. května 2019**

  
Prof. Ing. Zdeněk Peroutka, Ph.D.  
děkan



  
Doc. Dr. Ing. Vjačeslav Georgiev  
vedoucí katedry

V Plzni dne 5. října 2018

# Declaration of Authorship

I, Bc. Markéta BULÍNOVÁ, declare that this thesis titled, “Remote Monitoring of Animals Vital Functions by Using IoT” and the work presented in it are my own.

I confirm that:

- Where any part of this thesis has previously been submitted for a degree or any other qualification at this University or any other institution, this has been clearly stated.
- Where I have consulted the published work of others, this is always clearly attributed.
- Where I have quoted from the work of others, the source is always given. With the exception of such quotations, this thesis is entirely my own work.
- I have acknowledged all main sources of help.

Signed:

---

Date:

---

*“You become responsible forever for what you have tamed.”*

Antoine de Saint-Exupéry

ZÁPADOČESKÁ UNIVERZITA

## *Abstrakt*

Fakulta elektrotechnická

Katedra aplikované elektroniky a telekomunikací

Inženýr (Ing.)

### **Dálkový monitoring životních funkcí domácích zvířat s využitím IoT**

Bc. Markéta BULÍNOVÁ

Tato práce je zaměřena na návrh nositelného systému pro monitorování životních funkcí zvířat. Nejprve jsou v práci popsány systémy běžně využívané veterináři na jejich klinikách a dále jsou představeny dvě studie zabývající se bezdrátovými systémy pro zvířecí zdravotní péči, které nám nabízí dva různé pohledy na danou problematiku. Nakonec jsou v teoretické části práce představeny nízkoeenergetické sítě podporující přenos dat ze zařízení postavených na principu internetu věcí. Na základě informací získaných v teoretické části práce je navržen systém bezdrátového monitorování zdravotního stavu zvířat, konkrétně psů. Toto zařízení se skládá z pěti subsystémů, kde první monitoruje srdeční funkci zvířete na principu elektrokardiogramu, druhý snímá srdeční tep s využitím pulzního oximetru, třetí sleduje aktivitu zvířete pomocí akcelerometru, čtvrtý sleduje závislost povrchové a vnitřní teploty těla a pátý se skládá z přenosu dat ze systému na uživatelský cloud pomocí nízkoeenergetické dalekodosahové sítě. Každý navržený subsystém je v této práci otestován na konkrétním zvířeti z hlediska jeho skutečné využitelnosti a spolehlivosti pro systém dálkového monitorování životních funkcí zvířat.

#### **Klíčová slova**

pulzní oximetrie, elektrokardiogram, internet věcí, přenos dat, monitorování teploty, krokoměr

UNIVERSITY OF WEST BOHEMIA

## *Abstract*

Faculty of Electrical Engineering

Department of Applied Electronics and Telecommunications

Engineer (Ing.)

### **Remote Monitoring of Animals Vital Functions by Using IoT**

by Bc. Markéta BULÍNOVÁ

This thesis focuses on a design of a wearable system for remote monitoring of animal's vital signs. At first, the laboratory systems for animal health management utilized by vets have been introduced together with two studies dealing with wireless health monitoring of animals which indicate two different approaches to the animal health management. Finally, the low-power networks supporting IoT technology are introduced in the theoretical section of this thesis. Based on the knowledge from the theoretical thesis part, the wireless system which monitors the animal's, especially canine, vital functions is designed. This system consists of five subsystems where the first one monitors the heart functionality based on the principle of electrocardiography, second one deals with heart rate monitoring based on pulse oximetry, third subsystem monitors the animal's activity using an accelerometer, the fourth subsystem observes the animal's surface temperature with respect to its dependency on the animal's core temperature and finally, the last designed subsystem serves for low-power data transmission from the device to a user cloud. Each designed subsystem's functionality has been tested on a specific animal and its suitability for the animal health management has been clearly stated.

**Key Words** Pulse Oximetry, Electrocardiogram, Internet of Things, Data Transmission, Temperature Monitoring, Pedometer

## *Acknowledgements*

I would like to express my gratitude to my advisor Doc. Ing. Jiří MASOPUST, CSc. for his support of my work, valuable comments and supervision of this master thesis.

Moreover, I have to thank to MVDr. Kateřina Melicharová for consultations about the common animal welfare in veterinaries and to all members of my family for their continuous support of my studies.



# Contents

<b>Abstract</b>	<b>ii</b>
<b>Introduction</b>	<b>1</b>
<b>1 Animals' Vital Functions Monitoring</b>	<b>2</b>
1.1 Survey of Health Monitoring Systems . . . . .	2
1.1.1 Heart Rate Monitoring . . . . .	3
Pulse Oximetry . . . . .	3
Electrocardiography . . . . .	5
1.1.2 Temperature Scanning . . . . .	7
Veterinary Thermometers . . . . .	7
Temperature Sensors for IoT . . . . .	8
1.2 Researches of Wireless Health Monitoring Systems . . . . .	10
1.2.1 Wireless Canine Health Monitoring . . . . .	10
1.2.2 Cattle Wireless Behaviour Observation . . . . .	12
1.3 Summary . . . . .	14
<b>2 Communication Networks for IoT</b>	<b>15</b>
2.1 Low Power Wide Area Networks for IoT . . . . .	15
2.1.1 SigFox . . . . .	15
2.1.2 LoRaWAN . . . . .	18
2.1.3 Narrow Band IoT . . . . .	19
2.2 Short-range Area Networks for IoT . . . . .	21
2.2.1 WiFi . . . . .	21
2.2.2 Bluetooth Low Energy . . . . .	22
2.3 Summary . . . . .	24
<b>3 Thesis objectives</b>	<b>25</b>
<b>4 System Design</b>	<b>26</b>
4.1 Components . . . . .	26
4.1.1 ECG Electrode System . . . . .	26
4.1.2 Pulse Oximetry System . . . . .	27
4.1.3 Temperature Monitoring System . . . . .	28
4.1.4 Motion Activity Tracker . . . . .	29
4.1.5 Data Processing and Transmission . . . . .	30
4.2 Components Connection . . . . .	31
4.3 Sensor Deployment on Animal's Body . . . . .	32
<b>5 Designed Systems' Functionality</b>	<b>34</b>
5.1 ECG Monitoring System . . . . .	34
5.1.1 In-Vitro Experimental Analyses . . . . .	34

5.1.2	In-Vivo Experimental Analyses . . . . .	36
5.1.3	Final System Design . . . . .	37
5.2	PPG Monitoring System . . . . .	38
5.2.1	Hardware . . . . .	38
5.2.2	Experiment Set-Up . . . . .	40
5.2.3	Measured Data . . . . .	40
5.2.4	Measured Data Analyses . . . . .	41
5.3	Pedometer for Motion Activity . . . . .	44
5.3.1	Model Description . . . . .	44
5.3.2	Results Evaluation . . . . .	46
5.4	Surface - Core Temperatures' Dependency . . . . .	48
5.4.1	Wiring . . . . .	48
5.4.2	Experiment Set-up . . . . .	48
5.4.3	Measurement Results . . . . .	48
5.4.4	Equivalent Thermal Model . . . . .	50
5.5	SigFox Data Transmission . . . . .	52
5.5.1	Hardware . . . . .	52
5.5.2	Software Environment . . . . .	55
5.5.3	User Interface . . . . .	56
<b>6</b>	<b>Discussion</b>	<b>61</b>
6.1	Experiments Recapitulation . . . . .	61
6.2	Results Summary . . . . .	61
	<b>Conclusion</b>	<b>65</b>
	<b>References</b>	<b>66</b>

# List of Abbreviations

<b>ECG</b>	<b>E</b> lectro <b>c</b> ardiogram
<b>PPG</b>	<b>P</b> hoto <b>p</b> lethysmography
<b>IoT</b>	<b>I</b> nternet <b>o</b> f <b>T</b> hings
<b>LP-WAN</b>	<b>L</b> ow <b>P</b> ower - <b>W</b> ide <b>A</b> rea <b>N</b> etwork
<b>LAN</b>	<b>L</b> ocal <b>A</b> rea <b>N</b> etwork
<b>PAN</b>	<b>P</b> ersonal <b>A</b> rea <b>N</b> etwork
$SpO_2$	<b>P</b> eripheral <b>O</b> xygen <b>S</b> aturation
<b>LED</b>	<b>L</b> ight <b>E</b> mitting <b>D</b> iode
<b>IMU</b>	<b>I</b> nertial <b>M</b> easurement <b>U</b> nit
<b>CRA</b>	<b>Č</b> eské <b>R</b> adiokomunikace
<b>NB-IoT</b>	<b>N</b> arrow <b>B</b> and - <b>I</b> o <b>T</b>
<b>bps</b>	<b>b</b> its <b>p</b> er <b>s</b> econd
$T_a$	<b>A</b> mbient <b>T</b> emperature
$T_s$	<b>S</b> urface <b>T</b> emperature
<b>BLE</b>	<b>B</b> luetooth <b>L</b> ow <b>E</b> nergy
<b>SDA</b>	<b>S</b> erial <b>D</b> ata
<b>SCL</b>	<b>S</b> erial <b>C</b> lock
<b>sps</b>	<b>s</b> amples <b>p</b> er <b>s</b> econd
<b>bpm</b>	<b>b</b> eats <b>p</b> er <b>m</b> inute
<b>DMP</b>	<b>D</b> igital <b>M</b> otion <b>P</b> rocessor
<b>REPL</b>	<b>R</b> ead <b>E</b> valuate <b>P</b> rint <b>L</b> oop

# Introduction

The development of wearable devices for human health monitoring has been outspreading significantly for last several years. Recently, the idea of remote vital signs monitoring has become interesting for animal health management either, as animals are often treated as members of a family. A system, which could daily monitor their vital signs without disturbing them, would improve the human-animal interactions and more effective animal training could be achieved. The system would provide the owner an objective view of the animal's responses to specific situations so that the training of animals (e.g. racing horses or service/companion dogs) could be more adapted to the specific animal's needs. The vital signs' variations can be interpreted into animal's emotional responses to a current event or environmental condition, or it can serve as a health issues indicator so the owner can be alarmed.

The aim of this thesis is to design a system which could in real time monitor the animals' vital signs wirelessly without disturbing the animal at all. Such a device would provide more relevant results of conscious animals than the laboratory monitoring devices ever could because of the animal's stress caused by the measurement itself.

The designed system will be based on principles of veterinary systems commonly used by veterinaries for animal welfare in their practise and on studies [1, 2] which focus on similar objectives.

The designed system will contain the electrocardiogram (ECG) [1], photoplethysmogram (PPG), temperature monitoring sensors, activity tracking device and data transmission unit. Every system will be separately tested on a specific animal to determine its efficiency and potential utility in animal wireless health management.

## Thesis disposition

**In first two chapters** of this thesis, the current state of the art of animal health monitoring systems principles and the low-power consuming networks supporting Internet of Things (IoT) devices will be introduced.

**The third chapter** will summarize the thesis objectives.

**In the fourth chapter** the system for remote animals vital signs monitoring will be designed and **the fifth chapter** will demonstrate experiments observing the utility of the designed device's subsystems in the wireless animal health management.

**In the last chapter** the experiments' results will be evaluated and with respect to achieved results, a future system's enhancement will be suggested.

# Chapter 1

## Animals' Vital Functions Monitoring

This chapter introduces the current state of the art of animal's vital functions monitoring in the veterinary or laboratory environment and two studies which focus on the research of wearable systems for animals' health monitoring. Each of these studies offers a different approach to the animal welfare where both are interesting to consider.

The information about the animal health monitoring in veterinaries was declared by MVDr. Kateřina Melicharová, unless stated otherwise.

### 1.1 Survey of Health Monitoring Systems

It is logical that animals are not monitored so thoroughly as humans during surgeries or veterinary examinations, mainly in a small private veterinary practices. Simpler monitoring systems are usually utilized there, such as pulse oximeters with photoplethysmograms which monitor the oxygen saturation of blood. It is also quite common that they monitor the vital signs of the animals only visually (chest or inner eye movement) or by listening of animal's heart, using e.g. phonendoscope.

On the other hand, in bigger facilities, such as veterinary practise of MVDr. Michal Fiedler [3], there are more complicated and more accurate systems, such as electrocardiograms (ECG), X-ray or echocardiography (ECHO), commonly used for deeper medical check-ups. These systems are of course more expensive and they focus on the examination of specific heart diseases when there is already a suspicion that the animal suffers or could suffer (based on the breed and its congenital propensity to some cardiographic diseases) of a cardiographic abnormality. In case of some dog breeds, the ECHO, X-ray or ECG physical examinations should be performed preventively in the veterinary environment, because a wearable device for daily usage can never fully supplant a deep examination of a qualified vet (or doctor in general).

Furthermore, the respiratory rate monitoring is usually based on observing of the animal's chest movement whether it moves periodically, or by counting the breaths taken per minute. Therefore, it will not be included in this study in more details.

The basic principles of systems used for animals' vital signs monitoring in laboratories, which also have the potential to be incorporated in wireless wearable devices, are described below. This thesis focuses mainly on the temperature and heart rate monitoring as they serve as the main indicators of health abnormalities initials.

The standard ranges of the core temperature, heart rate and respiratory rate of cats, dogs, horses and cows are introduced below in Tab.1.1 when the animals are either sleeping or resting.

TABLE 1.1: Normal vital signs' ranges of temperature, heart rate and respiratory rate [16]

Animal	Temperature [°C]	Heart Rate [bpm]	Respiratory Rate [breaths per minute]
Cats	38.1 - 39.2	110 - 130	16 - 40
Dogs	37.9 - 39	60 - 140	18 - 34
Horses	37.2 - 38.1	32 - 44	10 - 14
Cows	36.7 - 39.1	60 - 70	26 - 50

### 1.1.1 Heart Rate Monitoring

As already declared, there are various options for heart rate examination. Most of them can be performed only in the laboratory environment as there are quite significant demands on the animal stillness and no motion activity at all. For example, the ECHO and X-ray examinations belong to this group as both require the animal to lay still. Moreover, the X-ray examination is out of option for its wearable device integration for its harmfulness when a body is exposed to the X-rays for too long. The ECHO examination can be considered as the essential examination method for a cardiographic patient as the heart can be observed in action. Hence, the heart blood pump ability can be checked, the heart valve damage can be revealed, etc. Contrariwise, the patient must lay still without motion to obtain relevant results. [3]

There are two main principles of heart rate monitoring which are applicable to wearable devices and which can deal with the animal motion activity.

First of them is called pulse oximeter. It utilizes the optical sensor and it is based on phyoplethysmography(PPG).[4]

The second system for heart rate monitoring is ECG which uses two and more electrodes to measure the voltage difference between them as a function of action potential transmission in myocardium.[5]

#### Pulse Oximetry

The pulse oximetry is based on the heart functionality. As the heart pumps, the blood volume in arteries changes. During the systolic phase, when the heart expels blood, the blood volume is bigger than when the heart draws blood during the diastolic phase. Due to this blood volume variation between these two phases, the optical absorption coefficient of the arterial layer changes and so does the amount of absorbed and reflected light.[4, 6]

Pulse oximetry offers two modes of use where in both PPG sensor optically measures the blood volume in arteries.

The **transmissive application mode** is more common for clinical utilization. In this case, an oximeter probe is clipped on a thin part of the animal body and two light wavelengths pass the animal's body part. The probe must be placed to hairless, minimal-pigmented body areas, such as tongue, lips, etc. The absorption variations of both

wavelengths are measured by the photodetectors placed in the opposite side of the reflecting photodiodes. The absorption varies according to the pulsing arterial blood and it is evaluated as the peripheral oxygen saturation ( $SpO_2$ ). The result of this monitoring is displayed as a percentage of oxygen saturation of hemoglobin, the blood protein carrying oxygen, in the arterial blood. The common ranges of the oxygen blood saturation are from 95% up to 99% for most animal kinds. Basically, there are two forms of hemoglobin. First of them is so called oxydized hemoglobin ( $HbO_2$ ) for the amount of oxygen it is carrying, the second one is deoxydized hemoglobin ( $Hb$ ) when the hemoglobin oxygen is exhausted. The  $SpO_2$  is the ratio of the  $HbO_2$  to sum both  $HbO_2$  and  $Hb$  which is presented in the following formula. [6]

$$SpO_2 = \frac{HbO_2}{HbO_2 + Hb}$$

In case of more advanced devices, the pulse rate can be displayed as a function of time.[6]

Two light-emitting diodes (LEDs) are utilized in the transmissive mode for either humans or animals. One LED emits the red light within wavelength of 660 nm and the second LED works with the wavelength of 940 nm, which is in the infrared range. These two wavelengths are absorbed differently during the systolic and diastolic phases, respectively the absorption differs with the amount of hemoglobin in the blood. When the blood is oxygenated (contains more hemoglobin), the infrared light is absorbed more than the red light, which passes through more easily. Oppositely, for deoxygenated blood more red light is absorbed and more infrared one passes through. Then, the difference of light absorption of both wavelengths is calculated and displayed as a percentage of  $SpO_2$ . [6, 7]

The spectrum of wavelengths, including red and infrared lights, is pictured in 1.1 as a function of blood absorption of either oxygenated or deoxygenated hemoglobin.

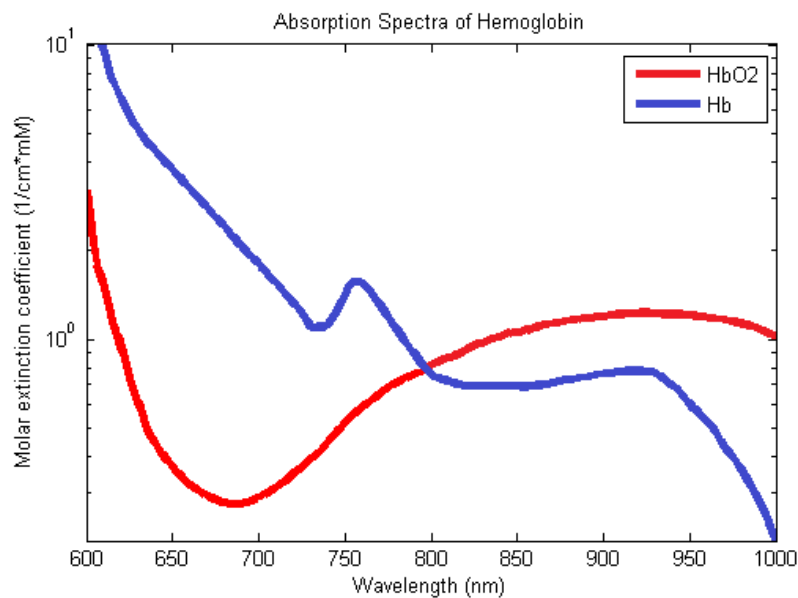


FIGURE 1.1: Absorption of oxygenated hemoglobin ( $HbO_2$ ) and deoxygenated hemoglobin ( $Hb$ ) as a function of wavelength [6]

The second mode of pulse oximetry is **the reflective mode**. The arterial blood volume is obtained by illuminating the body tissue and evaluating the back reflected light by

photodetector. The advantage of this method is that a thin patient body part is not necessary and the sensor can be placed on a feet, arm, forehead or thorax.[4, 6]

Therefore, the small wearable human wrist devices are capable of real-time heart rate monitoring. The reflective measurement is convenient for this heart rate measurement. A light source and a light detector are necessary in this application. The emitted light must pass through the skin, tissue and blood vessels (and fur, in case of animals). The light is then either absorbed, scattered or reflected back to the photodetector. Just a small amount of the emitted light is received back by the detector. The amount of reflected light differs according to the blood volume in the arteries, which changes with every heartbeat.[4]

The principle of reflective measurement is pictured in Fig.1.2.

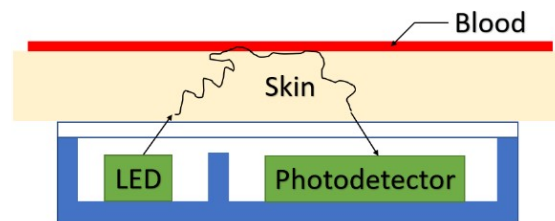


FIGURE 1.2: Reflective optical heart-rate measurement [4]

The heart rate measuring based on the PPG is already common in either laboratory (transmissive mode) or in human wearable devices (reflective mode). The impact of animal fur and body build can influence the performance of such devices, mainly in case of the reflective measurement where a thick body part is illuminated. On the other hand, it would be less invasive for animals to place the PPG sensor on their neck, for example, than on earlobe or tongue as it is in the transmissive mode of veterinary pulse oximeters. According to [4], when human body build is considered the peak absorption coefficient concur to the wavelengths of 540 to 570 nm, which correspond to the green light range. Therefore, for human wrist devices the absorption variation caused by the blood pump is the most visible when a light emitter works within these wavelengths, because the signal measured by the photodetector is the strongest one. On the other hand, the animal fur will play a big role in the light attenuation. Therefore, the LED and photodetector should be adapted by some light leading optical fibers to encourage the optical coupling of the incident light and the animal's skin. Contrariwise, the fur would have to be shaved to obtain relevant stable results.

## Electrocardiography

Electrocardiography is the main diagnostic method in cardiology based on the principle of heart activity scanning and the result recording. The heartbeat can be displayed on a paper or screen as the P-QRS-T waveforms where one P-QRS-T waveform represent one heartbeat (pictured on Fig.1.3). From the P-QRS-T waveform various heart diseases can be detected by a experienced doctor/vet.[5]

The electrodes are placed directly on the skin and the voltage differences between electrodes are measured as a function of myocardium active potential. Due to the active potential transmission in myocardium, the local electrical currents originate in the areas of different potential interfaces, which lead to the origin of electromagnetic field. The



body fluids work as good conductors which allow us to monitor the differences of cardiac potentials from the body surface. As the heart electrical activity is dependent on the mechanical heart functionality, ECG is an important diagnostic tool for various heart diseases. [5]

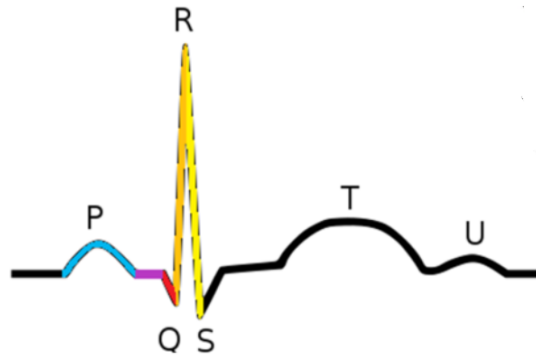


FIGURE 1.3: Representation of one heartbeat in ECG [5]

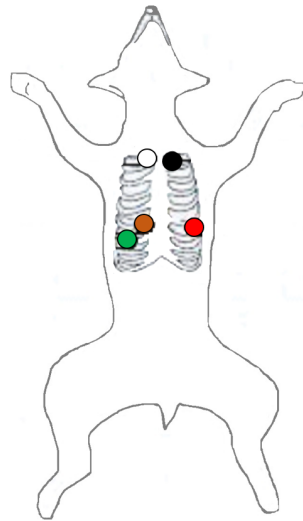
The electrocardiographic clinical examination is usually performed to detect even the smallest disturbances (arrhythmias) in the heartbeat. It can also detect the heart enlargement (cardiomegaly). The suitable treatment can be proposed when the correct diagnose is determined. In case of the veterinary environment the electrodes are attached with the crocodile clips directly to the skin of the animal's elbows and knees or on its chest while the animal is usually lying on the right side (or standing) full aware. The animal is usually not sedated during the clinical examinations, which takes only few minutes, as the chemical restraint could influence the obtained results, but the animal should not move. To improve the electrical conduction between the electrodes and animal's skin, the attachment areas are usually wetted with conductive liquid. The number of leads differs according to the used ECG machine. Some ECG systems include only four limb leads while others add some thorax leads either. In case of canine ECG monitoring the total number of leads is eight (four limb and four thorax leads) while not all of them have to be used. [3, 8]

In some cases there is a need of more thorough monitoring where the animal is observed for longer time than a regular vet check-up takes and during its daily routine. That is because during the ECG examination in the veterinary practise the heart rate abnormalities do not have to occur.

The Holter device can be used to monitor the animal for several hours or days, where the data are saved in a memory and post-processed. The Holter monitor can lead to serious heart diseases detection which an ordinary electrocardiograph could not find. [9]

Series of electrodes are attached to the patient's thorax on shaved spots and the Holter monitor records the electrical impulses produced by heartbeat. The electrodes are attached over bones so that the artefacts caused by muscular activity would be reduced. The number of electrodes is also from three up to eight and they are connected to microcontroller which is attached to the animal's chest belt. The Holter monitor is usually required when a heart rhythm incompatibility is detected via normal electrocardiograph to determine the exact nature and origin of the problems. [9]

The example of Holter monitor electrodes placement for canine heart rate monitoring is pictured in Fig.1.4a, although a different number of electrodes can be placed. In Fig.1.4b, there is a picture of a dog wearing the Holter monitor.



(A) Five-lead Holter monitor electrodes placement for dog



(B) Picture of a dog wearing the Holter device

FIGURE 1.4: Holter device ECG monitoring [3, 10]

The Holter monitor can be a useful tool for more accurate diseases detection and for continuous heart rate scanning. The heart activity is usually monitored continuously for 24 hours by the device and the results are saved in a memory to be later reviewed by a vet. The result evaluation can take even up to 3 days. [3]

The Holter monitoring device serves as a very good reference for any heart rate monitoring wearables under development to verify the results.

Contrariwise, the ECG monitoring devices manufactured by e.g. Polar can serve for heart rate monitoring of animals under an endurance training. These devices are sometimes used by professional horse riders to monitor the horse's heart rate continuously during the training because the horse's heart rate at rest and after the practise is one of the qualification criterion for several horse races and it must retain below specified level so that the horse could contest. On the other hand, such devices, which are usually attached to the animals belly under the horse saddle belt, can scrape the animal. Therefore, most of the riders prefer to monitor the heart rate before and after the practise by simple counting of the beats in a minute.

### 1.1.2 Temperature Scanning

In the veterinary, core body temperature of animals is usually measured rectally, because the surface temperature varies a lot during the day according to the animal's activity or the ambient temperature.

#### Veterinary Thermometers

The temperature sensing in IoT devices can be provided by various sensors, but the most common veterinary thermometers are digital thermometers using infrared radiations for contactless or in-ear measurements or mercury thermometers based on rectal temperature measurement.[11]

The different types of animal's thermometers are described below.

- *Mercury thermometers*

The mercury thermometers are formed of glass bulb which contains mercury in a glass tube of smaller diameter than the bulb has. The mercury does not cover the whole volume of the narrow tube, but it changes its volume depending on the temperature. The mercury thermometers usually measure the animal temperature rectally, which is more disturbing for the animal than the in-ear or contactless thermometers. The medical usage of the mercury thermometers can be very accurate, but in some countries the mercury thermometers are forbidden to use for medical body temperature measurement because of the toxicity of mercury. [11]

- *Non-touch thermometers*

The contactless thermometers are based on the principle of black body radiation. Accordingly, any material with temperature above the absolute zero contains moving molecules in it which emit infrared radiation due to their movement. The molecules' movement speed depends on the material temperature. The higher the temperature rise, the faster the molecules move and the more radiation they emit. The non-touch infrared thermometers detect and measure the emitted radiation of the materials.[11, 12]

The infrared thermometers contain lens to focus the infrared light from the specific object onto a thermopile, which is an infrared light detector. The thermopile absorbs the infrared object radiation and the more radiation it absorbs the hotter it gets. The thermopile excess heat is then converted to electrical energy which is analysed by an electrical detector and the object temperature is determined.[12]

These thermometers are risk-free for the animal temperature monitoring as they do not contain any mercury. Moreover, the temperature measurement is very fast (takes only few seconds to measure) and non-invasive and non-stressful for the animal at all. The temperature is typically measured on the animals underbelly where is less hair than elsewhere.[12]

- *In-ear thermometers*

The in-ear thermometers are less intrusive than the rectal thermometers, yet they require contact with the animal skin to measure the temperature. They can be based either on the infrared radiation measurement, which focuses on the infrared waves coming out of the animal's eardrum, or they can use mercury. The temperature measurement must follow strictly the instructions provided by the manufacturer to obtain accurate results because the right part of the animal ear must be targeted.[11]

## **Temperature Sensors for IoT**

Unlike the above described thermometers, there are temperature sensors which could be used for IoT devices to measure either the animal's surface temperature or the ambient temperature or both. Therefore, the owner can be alarmed when the animal would be overheated or hypothermic.

The principles of some temperature sensors, which could be potentially implemented for the wearable temperature monitoring device, will be described below.

- *Thermistors*

Whereas the resistance of thermistors is dependent on the temperature of their immediate vicinity, the thermistors are highly temperature sensitive devices. They are very

sensitive to the ambient temperature changes. In case of even the smallest temperature variation, the resistance changes significantly. [13]

The most common materials for the thermistors are semiconductors, such as oxides of chromium, cobalt, nickel, manganese and sulphides of iron, aluminium or copper. [13]

- *Resistance Temperature Detectors (RTD)*

The RTD sensors contain a sensing element, usually produced from a pure metal, which resistance also changes with temperature. The most common used materials are platinum, nickel or copper and they can be processed either as a thin film or wired. The RTD resistance is determined from an applied constant current and the measured resulting voltage. RTD sensors bias to use a constant current source and the current magnitude is set to be low as much as possible to reduce the self-heat caused by power dissipation.[14]

- *Digital Temperature Sensors*

The digital temperature sensors benefit from the non-necessity of any extra components, such as A/D converter, etc., as they already provide the digital information about the temperature in degrees Celsius. It is so because they already integrate all those function for which the thermistors and other analogue thermometers require the external handling. The output of the digital sensor is a digital reading of various bit accuracy (e.g. 9 to 12-bit temperature measurement of DS18B20 thermometer). [14, 15]

Moreover, some of the digital temperature sensors, such as the DALLAS DS18B20 thermometer, benefit from a matter of fact that each device has its own 64-bit serial code which is stored in a ROM memory. This feature allows the users to connect multiple DS18B20 devices in parallel on the same 1-Wire bus. [15]

## 1.2 Researches of Wireless Health Monitoring Systems

The animals vital signs monitoring wearable devices are not so common on the market. There are only few manufactures who provide the wireless vital signs monitoring system for animals. For example, the PetPace animal collar is a commercial device which covers our demands for the animal health monitoring system which includes the heart rate monitoring and temperature scanning. On the other hand, there is very limited information available about the technologies they implement and the reliability of their device. The only information cleared from their website <https://petpace.com/> is that the animal core body temperature they declare to be observing by the device is only estimated from the ambient temperature and animal activity to be *low*, *normal* or *high*.

There are various scientific studies about wireless animal health monitoring, but these systems usually are not available on the market. Two studies concerning with the animal health management will be described below, each section will be based on one study presented in the cited scientific journal.

### 1.2.1 Wireless Canine Health Monitoring

This section of the thesis is all based on the study of [1].

The aim of the authors was to create a system which could continuously monitor the canine vital functions outside of the laboratory so that the link between physiological signs and the emotional states of dogs could be identified. The final device combined ECG, PPG and inertial measurement units (IMU) to gain the information of canine real-time vital signs remotely.

Due to the impact of the canine skin and dense hair layers, they performed a research which examined various styles of ECG electrodes and also the influence of conductive polymer coatings of the ECG electrodes to determine the best solution for the system. The efficiency of the optical coupling of PPG sensors to the skin was also under the research.

The authors wanted to avoid shaving the canine hair and also they aimed to develop a system which would be comfortable for the animal to wear and easy to use for the dog's handler. Based on these demands, the ECG electrodes, traditionally used in veterinary clinics, were inapplicable, because they would be painful or highly uncomfortable for a moving animal.

In order to determine the best ECG electrode system for the canine heart rate measurement they performed research which required the *in vitro* and *in vivo* impedance analysis of the examined electrodes (spring-loaded pin arrays) and the electrodes used at clinics (stainless steel electrode). The *in vitro* analyse examined a) the impact of metal electrode surface modification by coating with poly(3,4-ethylene-dioxythiophene) poly-(styrene-sulfonate) (PEDOT:PSS) conductive polymer to the impedance of tissue-electrode interface and b) the quality of the examined electrodes tissue coupling. The *in vivo* analyse involved a) the comparison of the ECG system with a Holter monitor which can be used for wireless ECG monitoring and b) the reliability of the ECG when the dogs were doing their routine activities.

The *in vitro* analysis showed the impact of the number of pins of the spring-loaded gold-coated pin arrays to the overall electrode impedance at the frequency range of 10 Hz up to 10 kHz. Fig.1.5a shows that both electrode types demonstrated similar impedance,

but when the number of pins of the pin array electrode was incremented its impedance decreased. Unfortunately, the penetration through the hair become more challenging when additional pins were added. Therefore, when the pins quantity per electrode was chosen a compromise of the tissue-electrode impedance decrease and the simplicity of fur penetration had to be done.

On the other hand, the effect of PEDOF:PSS coating over the gold coated spring-loaded pin arrays is demonstrated in Fig.1.5b. The impedance decreased significantly mainly for low frequencies which are typical for heart-rate. The impedance of a single pin lowered from  $4.8\text{k}\Omega$  to  $670\Omega$  at  $10\text{ Hz}$  and for a four-pin array it lowered from  $2.3\text{k}\Omega$  to  $300\Omega$  at the same frequency.

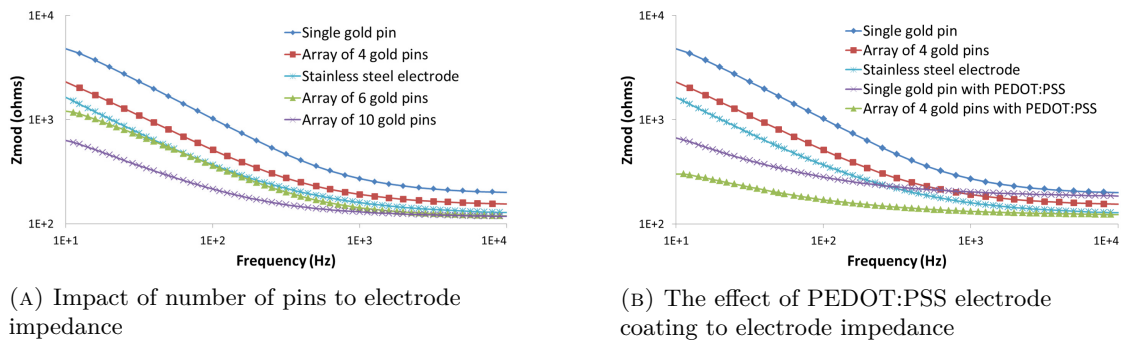


FIGURE 1.5: In vitro EIS measurement [1]

The in vivo measurement was performed to determine the system's accuracy when the results were compared with the Holter monitor introduced above. Moreover, the system reliability test was executed when the animal was monitored during activities of various intensities. The intensity level was observed by the set of accelerometers. For the system analyses and the final system design refer to chapter 5.1, where the ECG heart rate monitoring system designed by [1] is described in more details.

Moreover, they included PPG sensor to aim heart rate and heart rate variability self-calibrating measurement. The traditional PPG recording might be used only on anesthetized animals during surgeries or motionless animals because the pulse oximetry clips are attached to the animal's tongues or ears. The authors used the  $850\text{ nm}$  IR LED diode to illuminate the canine tissue on the dog's thorax and they tried to deal with the dense animal hair layers by implementing, for both LED and photodetector, the light fibers to improve the optical coupling with the canine skin. The impact of optical fibers was studied to achieve an efficient optical coupling to canine skin through the hair on their thorax in case of PPG measurement. The sensors were placed on thorax mainly because the chest belt does not restrict the animal to move at all. When the animal lays still, the PPG and ECG heart-rate measurements can be compared to validate the measurements accuracy. On the other hand, during any animal motion activity the signal from the PPG method degrades significantly.

The principle of the PPG heart rate measurement and the optical coupling to skin by using the light guides and light fibers is pictured in Fig.1.6.

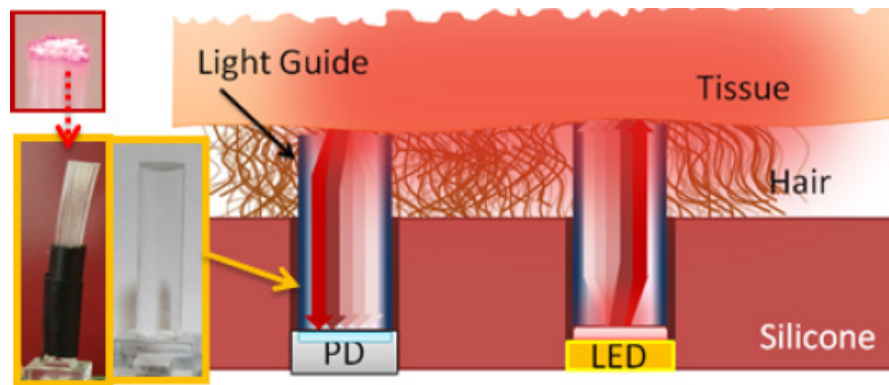


FIGURE 1.6: The PPG heart rate measurement [1]

The obtained data were processed and transmitted to owner's device by a wearable BeagleBone Black processing unit. The communication was based on the IEEE 802.11 standard for Wi-Fi or for scenarios where Wi-Fi is not available the Texas Instruments system-on-chip (cc2541) for Bluetooth communication was included to connect with the owner's device.

### 1.2.2 Cattle Wireless Behaviour Observation

This part of the thesis is all based on the study of [2].

Their study describes the set of experiments in which the cattle behaviour was observed using collar, halter or ear tag sensors. A machine learning algorithms were integrated to classify the obtained data to specific behaviour classes, such as grazing, standing, resting, walking, ruminating and other.

Two different approaches for the behaviour classification model based on the collected data from all three locations were executed. First of them trained on the data from a sample of animals while the model was then tested on a different sample of animals. The second model mixed data from all animals, trained the algorithms on data of a part of mixed data sample and then tested the model on some animals from the data sample. Usually, developing of standard behaviour models includes so called 'windowing' which partitions time data into short time windows and extracts a set of statical features. The classifier training combined the statical features with the corresponding behaviour class with high accuracy. The Discrete Fourier Transformation (DFT) was performed to obtain the frequency domain representation of the time series data. The motion intensity was represented by the standard deviation, minimum and maximum features.

The standard scope of the cattle behaviour classifier is presented in Fig. 1.7.

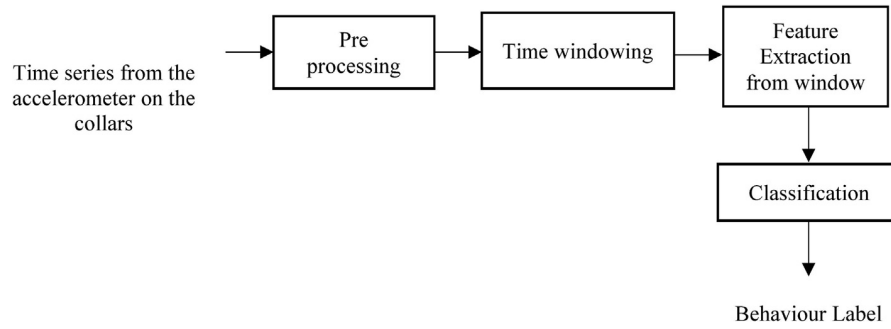


FIGURE 1.7: Scope of cattle behaviour classification [2]

The main aim of the study was to determine the impact of sensors placement to the behaviour classification accuracy. Hence, the collected data were from accelerometers placed on *a)* neck (collar), *b)* head (halter) and *c)* ear (ear tag). The results of the animal observation from all three body parts are plotted below in Fig.1.8.

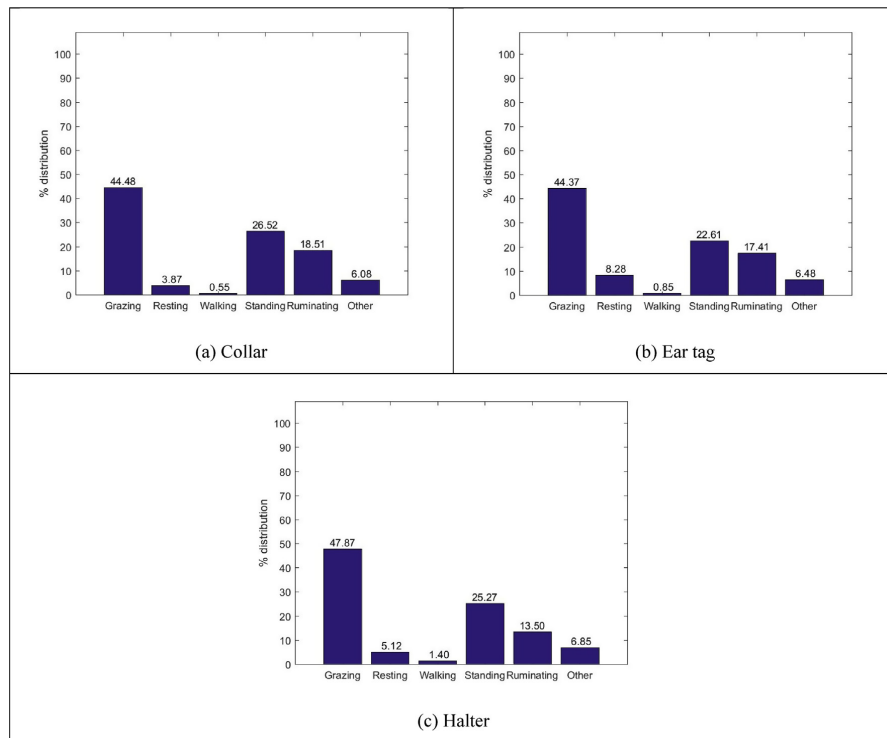


FIGURE 1.8: Class distribution from data sets from collar, halter and ear tag collected from all observed animals [2]

As it is visible from the figure above, classes 'resting', 'walking' and 'other' are represented by the smallest amount of time. Hence, the authors decided to discard these three classes from the observation. Moreover, according to various validation approaches the authors used for the data evaluation, the halter data showed to be the most accurate from all three observed spots of animal body.



### 1.3 Summary

This section of the thesis described the current state of the art of systems used in veterinary clinics and two studies of different approaches to the animals' health management.

The heart rate monitoring and the core temperature observation are the most common vital signs monitored by vets. Above described systems introduce their functionalities and prime principles of the animals' vital signs monitoring. Some of them, such as ECG, are already commonly used for wireless heart functionality monitoring by so called Holter monitors, which serve as a long-term continuous heart rate monitoring during patient's daily activities to determine heart's abnormalities more precisely than during a veterinary examination. Nevertheless, the electrodes' sizes and shapes can be adapted so that the animal fur does not have to be shaved which was proved by the [1]. Therefore, the ECG system can be integrated in the final system design.

Furthermore, the PPG systems are integrated in human wrist devices for heart rate monitoring commonly which indicates the pulse oximetry's potential for its further utilization in animal's health management if the fur barrier is solved.

The core temperature continuous monitoring cannot be based on the thermometers described in chapter 1.1.2 due to their prime principles and the animal's body spots required for measurement. Nevertheless, the animal's surface temperature dependency on its core temperature could be observed to find a solution of animal's temperature monitoring for wearable systems.

Finally, the system introduced by [2] opens an interesting idea of undirect animal's health monitoring by observing their daily routine and the levels of various activities per day. If an activity decreases significantly compared to a common level, it can be an indicator of an illness or infection.

## Chapter 2

# Communication Networks for IoT

The idea of internet of things technology is to transmit a small amount of data with a low transmission speed, low energy consumption of the end devices and over long distances. Thus, a special kind of communication networks, in general known as LP-WAN (Low Power Wide Area Network), has been developed to support this new technology.[17]

In the Czech Republic, three main IoT communication networks are supported by various providers. First of them is supported by SimpleCell company providing the SigFox network based on the infrastructure built by T-Mobile. The second provider is company called České Radiokomunikace (CRA), which is part of the worldwide LoRa Alliance, with their LoRa (Long Range) network and finally, the mobile operators Vodafone and O2 provide the network based on the NB-IoT (Narrow Band IoT) technology within their LTE and 5G networks (able to work within 2G/3G network spectrum, too), which benefit from the existing infrastructure and the network inclusion into already exploited licensed spectrum.[17]

### 2.1 Low Power Wide Area Networks for IoT

LP-WANs are wireless communication networks developed to fill the gap between mobile networks and short-range networks, such as Bluetooth or WiFi, and to support the IoT technology. While the mobile networks are too expensive for IoT and the transmission rates unnecessarily high, the short-range networks are limited by the range they can cover. The LP-WANs are suitable for the IoT technology for the high coverage range, low transmission rates and low energy consumption of the end devices. [18]

#### 2.1.1 SigFox

The main provider of the SigFox network in the Czech Republic is the SimpleCell company which was also the first public provider supporting IoT. They built the network based on the infrastructure of T-Mobile, Czech provider of mobile services, where the base stations for the SigFox network are located. Generally, the SigFox company itself is the global IoT network provider, while SimpleCell manages the SigFox network in the Czech Republic.[17]

The SigFox network works within the license-free frequency band of either 868 MHz or 915 MHz, but the terms set by the Czech Telecommunication Office must be fulfilled. One of the terms is built on the amount of allowed transmitted messages per day within the network, which is 140 12-byte payload messages per day, and the low transmitting

power, which is either 100 or 600 mW depending on the region. The range of one base station is 30-50 kms in rural areas and from 3 up to 10 kms in urban areas. On the other hand, for most IoT devices the SigFox network is very suitable for the low energy consumption and low initial costs of the devices. The SigFox network is most commonly integrated in devices which transmit a small amount of messages per day or which do not require real-time continuous monitoring. Hence, most of the smart household monitoring devices or smart-city devices use the SigFox network.[19]

The UNB (Ultra Narrow Band) D-BPSK modulation is utilized for the uplink data transmission over SigFox. The network takes benefits from the high spectral efficiency of the D-BPSK modulation which allows to have only 1 Hz of transmission bandwidth to the transmission speed of 1 bit/s (bps). The energy concentration of the signal to the narrow band provides a high robustness against interferences and hence, the base stations can easily demodulate the signal despite the interferences. The base station receiver sensitivity is based on the transmission bit rate. The receiver sensitivity is -142 dBm for 100 bps bit rate and -134 dBm for the bit rate of 600 bps. Therefore, a large link budget is offered by the network due to the high receiver sensitivity. [20]

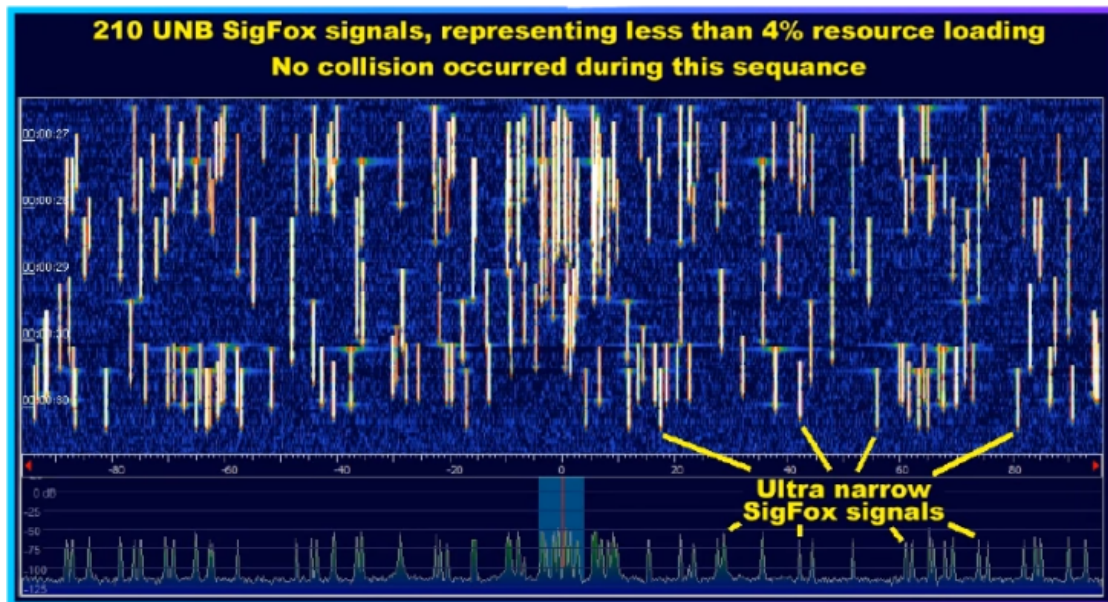


FIGURE 2.1: Spectrum analyses of 210 UNB SigFox signals [20]

The spectrum analyses of 210 UNB SigFox signals' transmission performed by [20] is plotted in Fig.2.1. The signals represented in the spectrum occupy only 4% of the radio resource and no signals' collisions occurred during the test where 200 kHz of operation band was covered. On the other hand, the conventional wireless system spectrum analyses performed also by [20] introduced that during the 13 GFSK signals' transmission within the 200 kHz 3 collisions occurred. [20]

Moreover, to extend the battery life as much as possible and to increase the network capacity a lightweight protocol has been introduced by SigFox. The total SigFox frame take 26 bytes in maximum for 12 bytes data payload. For comparison, the IP stack includes 40 bytes header for only 12 bytes of transmitted data. Thus, more efficient frame optimizes the battery life and provides more capacity for the data (refer to Fig.2.2). [20]

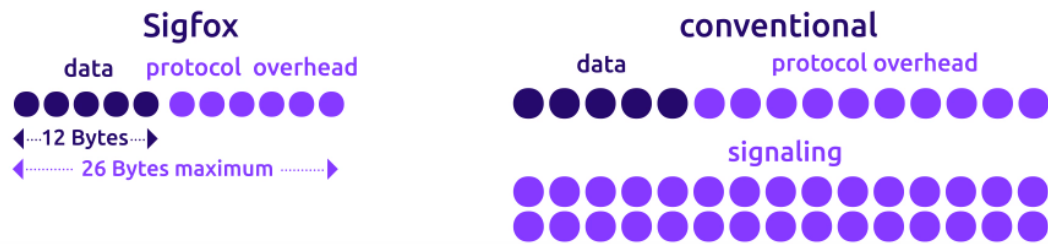


FIGURE 2.2: The SigFox and conventional protocols [20]

The data volume for uplink communication is from 0 up to 12 bytes with maximum 140 messages/day. When a message of 0 data bytes is sent, the message itself is considered as an identification of the device functionality. The downlink communication is limited to 4 messages/day of data from 0 up to 8 bytes. The downlink can be demanded by a user to e.g. request additional data or to adjust messages frequency.[20]

The SigFox devices do not communicate with only one base station at time like the cellular networks do. Each device broadcasts the messages and all base stations within the range receive it. On average, three base stations receive the message from the same device. It takes approximately 2 seconds for the message to reach the base station which then transmits the data to a SigFox cloud via point to point secured IP link. The access to the central SigFox cloud is provided to each user who gets sign-in and development tools to an application interface (API) are available. The users can develop their own applications there. [20]

The SigFox network architecture is shown on the Fig.2.3.

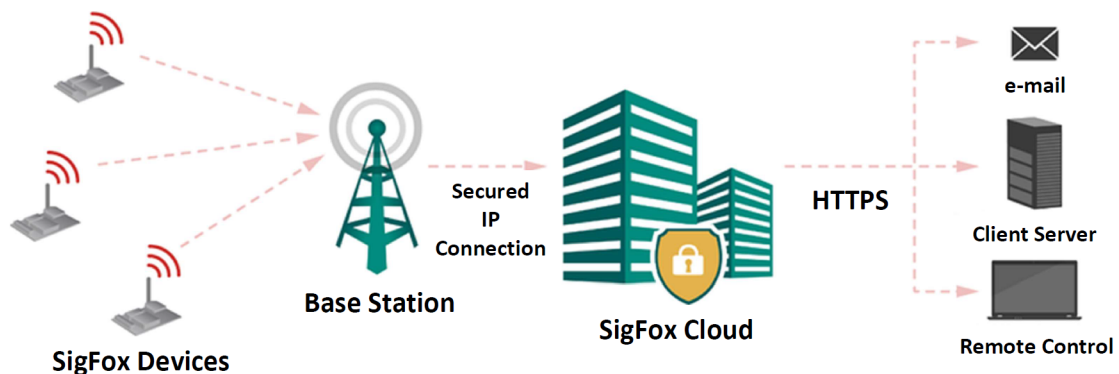


FIGURE 2.3: The architecture of the SigFox network [17]

Currently, the SigFox population coverage is 96% and the SigFox area coverage, pictured in Fig.2.4, is 94% in the Czech Republic. The big advantage of the SigFox network is that the indoor coverage is very good as well.

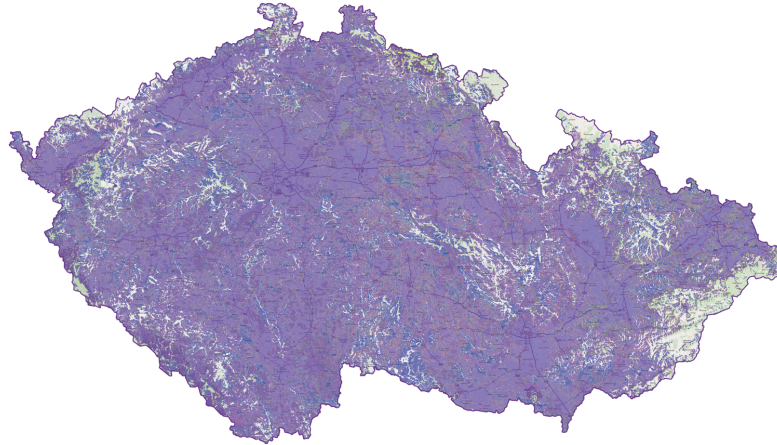


FIGURE 2.4: SigFox coverage [21]

### 2.1.2 LoRaWAN

The LoRa network was built by CRA to support the IoT technology as an access point of bi-directional radio communication. CRA benefits from their existing communication infrastructure which they only expanded for the LoRa Gateway base stations. Unlike the SigFox network, LoRa was created by a group of providers, so the costumers can profit from the advantage of more components produced by various manufactures. Nevertheless, only the certified devices can be logged into the LoRa network. [17]

LoRa, same as SigFox, network supports the IoT technology as it transmits a small amount of data over long distances with low energy consumption and low operating costs using the principle of radio wavelengths transmission with the usage of Chirp Spread Spectrum (CSS) modulation. The CSS modulation linearly spreads the signal to the entire transmission channel, which decreases the cost of the local oscillator due to lower demands on the frequency stability. Also, the chirp spread signal is highly robust to channel noise and multi-path signal transmission. Moreover, the device battery lifetime can be up to 10 years depending on the device functionality, amount and size of sent messages per day, etc. The LoRa bit rate is from 300 bps up to 50 kbps and in Europe it works within the non-license band of 868 MHz, same as the SigFox network. Following the LoRaWAN protocol, each end device can be configured according to the required data transmission rate and transmitting power and so, the battery life-time can be maximized for every device. The transmission bandwidth directly depends on the transmission rate and can be set from 7.8 up to 500 kHz. [17]

The LoRaWAN specification is a communication protocol for the LoRa devices and the LoRa Gateway stations. Each LoRa Gateway requires either its own dedicated connection or the secured connection from gateway to control server via the Internet. The server controls and dynamically changes the communication parameters for the gateways. Moreover, it monitors the state of entire network including the operating information of the end devices. It directs the messages to the requisite application server and it ensures that only the required user will receive the message. The IoT devices communicate using LoRa network up to nearest LoRa Gateway, wherefrom the data are sent via mobile network or Ethernet to superior server or cloud. Here, the data can be processed and made available for the end user over a website or mobile application. [17]

The LoRa network architecture is pictured in Fig.2.5.

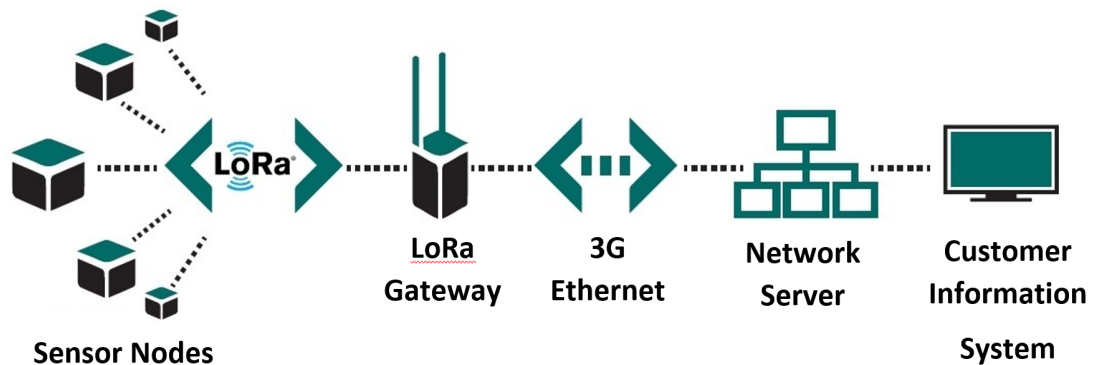


FIGURE 2.5: The LoRa network architecture [17]

The area coverage of the Czech Republic by LoRa WAN is shown in Fig.2.6. The CRA provides the LoRa network in all district cities and it ensures that they keep improving the area coverage by the network. [22]



FIGURE 2.6: LoRa WAN coverage[22]

### 2.1.3 Narrow Band IoT

The NB-IoT is a wireless licensed narrow band LP-WAN network developed for the IoT devices working within either the GSM (Global System for Mobile communications) or LTE (Long Term Evaluation) network. There are two technologies based on the LTE standard. First of them is called LTE CAT M1 (LTE-M) which uses the frequency band of 1.4 MHz with the transmission rate up to 1 Mbps and latency of 15 ms. The LTE-M is suitable for the wearable devices, security systems, etc., and it supports the Voice Over LTE (VoLTE) technology. The second LTE based technology for IoT is LTE Cat NB1 (NB-IoT). NB-IoT works within the frequency band of 200 kHz with the transmission rate of hundreds of kbps and the latency of from 2 up to 10 seconds. The NB-IoT is supported by the providers of mobile networks in Europe and Asia, while in the USA they choose the LTE-M. [19, 18]

The NB-IoT is supported by two mobile service providers, O2 and Vodafone, in the Czech Republic. The main advantage of the technologies in licensed frequency band is

their better change adaptation (scalability), good quality of services and high security management. The good scalability of the network is caused by the matter of fact that almost no additional hardware is needed to be installed. The software of the LTE transmitting stations is adapted so that a part of the frequency band would be reserved for the NB-IoT. [17, 18]

The area coverage is declared by Vodafone to be almost 100% while the inner space of buildings is covered from 94%. [23]

The end terminals transmit (receive) the data from the nearest NB-IoT Gateway from where they transmit the data to superior server/cloud where the data can be stored, processed or made available for the end user. The NB-IoT network architecture is pictured below. [17]

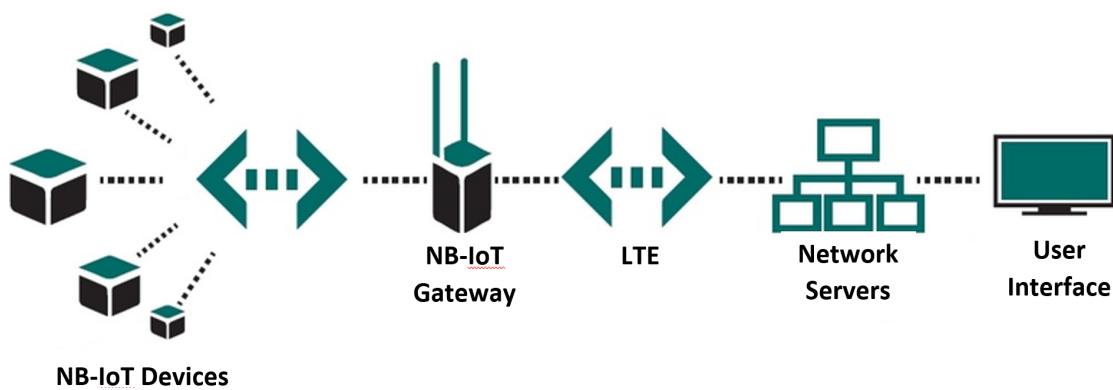


FIGURE 2.7: NB-IoT network architecture [17]

The number of the end terminals for the NB-IoT can be up to 200 000 devices for one network cell, because each device generates only small amount of data. The idea of IoT technology is to cover even the most distant areas for a long time, hence a low channel attenuation and low energy consumption is demanded.

As already mentioned, the NB-IoT system is based on the LTE standard, which means that for the downlink there is used the same OFDMA (Orthogonal Frequency-Division Multiple Access) access for both in the physical layer. The subcarrier spacing is  $\Delta f_c = 15$  kHz. The channel coding, transmission rate, interleaving and others are the same as in the LTE standard for the NB-IoT. The uplink uses the single tone transmission of either 15 kHz or 3.75 kHz. The upper layers such as RLC (Radio Link Control), MAC (Medium Access Control) and RRC (Radio Resource Control) are similar to LTE layers, but the access methods and security channels are special for the NB-IoT. The link budget of the NB-IoT network is 20 dB better than the link budget of LTE-A network, which allows to increase the area of undeveloped landscape coverage seven times or to compensate the attenuation of shaded areas. The link budget improvement is caused by the utilization of BPSK/QPSK modulations and the Automatic Repeat Request (ARQ) coding, by the enhancement of the Forward Error Correction (FEC) codes and the antennas space diversity systems (SIMO/MIMO), etc. [19]

The band width for either uplink or downlink is 200 kHz which reduces the transmission rate in the physical layer to 100-200 kbps. On the other hand, more terminals can work in parallel in case of a slow data rate. Moreover, the hardware, such as the A/D or D/A converters and additional circuits, can be simplified which lowers the power consumption and the price of the end terminals. [19]

Although the NB-IoT system is not directly compatible with the LTE/4G or 2G/3G networks, it coexists with these networks in the frequency band. There are three approaches of the NB-IoT and mobile networks coexistence. First of them is so called *Stand Alone Channel*, which is integrated in case of NB-IoT application to GSM/GPRS standards. These standards work within the frequency bands of either 900 MHz or 1800 MHz with the each channel band width of 200 kHz. The second one works within the LTE standard as so called *In-band* adaptation, where segments of the 180 kHz, intended for the resource block (RB) inside of a LTE channel, can be adapted for NB-IoT. The third option uses so called *Guard band* between two LTE channels. [19]

The demonstration of the NB-IoT coexistence options is pictured in Fig.2.8.

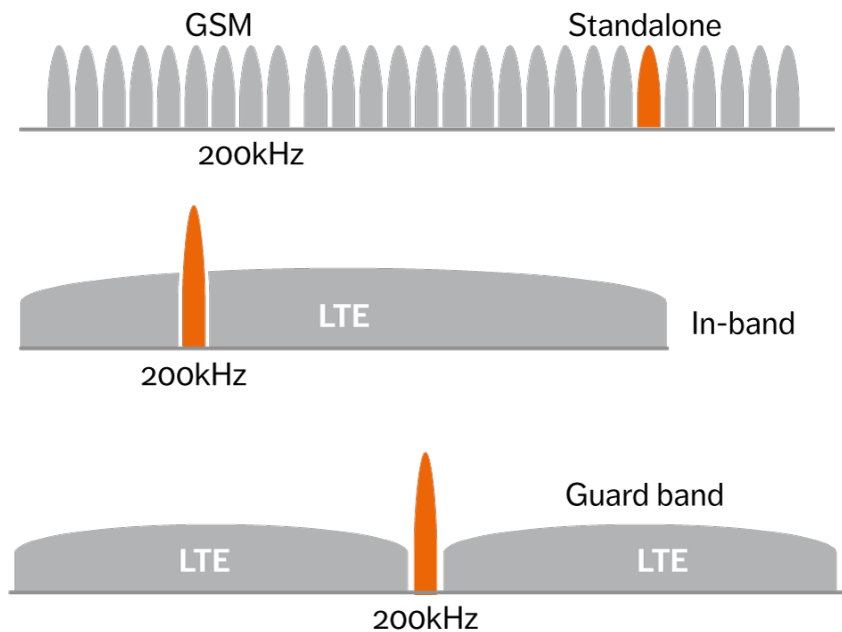


FIGURE 2.8: NB-IoT network co-existence with LTE/GSM [19]

## 2.2 Short-range Area Networks for IoT

The wireless local/personal area networks have been a logical choice for the IoT systems from the prime beginning for their ubiquity. Nowadays, most of the households are equipped with the WiFi router working within the wireless local area network (WLAN) and almost everyone in the world owns a device containing Bluetooth network which is part of the Wireless Personal Area Network family.[19]

### 2.2.1 WiFi

The most common WLAN networks based on the IEEE 802.11 standard work on the frequencies of 2.5 GHz and 5 GHz with channel bandwidth from 20 up to 160 MHz. Hence, the transmission rate for this network type is much higher than in case of the LPWAN networks. On the other hand, the range of one router coverage is around hundreds of meters maximally. [19]



Although the data rate and the coverage of the network is not very suitable for the IoT technology, there are some variations of the IEEE 802.11 standard, such as the 11a, 11b, 11ac, etc. standards. Some of them are adapted to fit the IoT demands better. For example, the IEEE 802.11ah standard works on a frequency lower than 1 GHz with narrow band of 1 or 2 MHz, which provides a higher range (up to 1 km) and support for many devices connected at once at the expenses of transmission rate. The 802.11ah standard is suitable for e.g. extensive sensor networks. [19]

The examples of 802.11ah standard utilization are pictured in Fig.2.9.

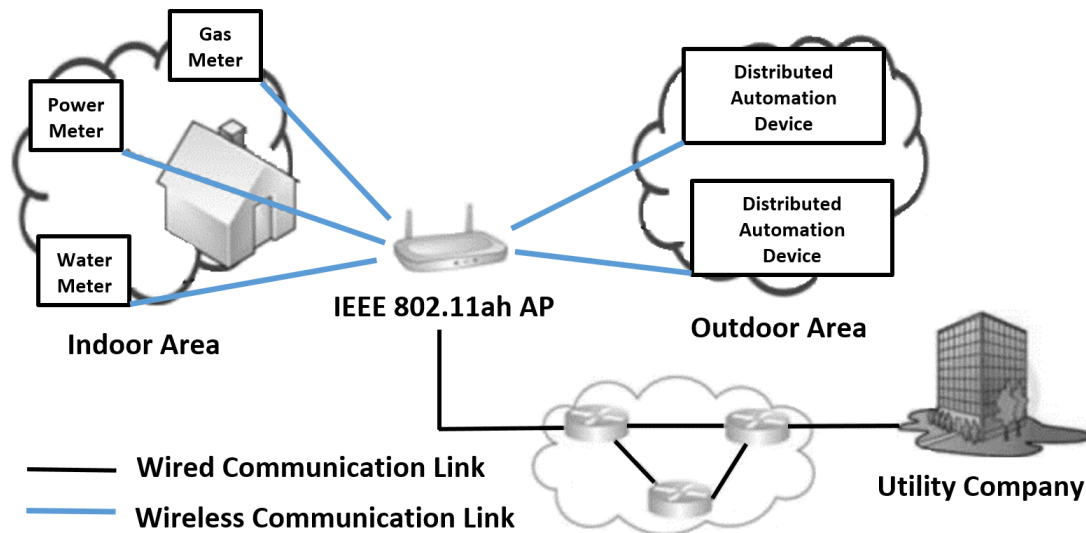


FIGURE 2.9: IEEE 802.11ah standard application [19]

## 2.2.2 Bluetooth Low Energy

The classical Bluetooth network belongs to a family of Wireless-PAN Networks and serves for short range data transmission. The Bluetooth Low Energy (BLE) is a low power-consuming version of Bluetooth Classic for IoT. The BLE technology is adapted to lower the power consumption of user terminals and to simplify the identification of the user device. Also the BLE topology is more convenient for IoT technology. Beside others, the end-devices power consumption is reduced by sleep-time extension and by modification of the communication protocol. [19]

The Bluetooth consists of one or more 'piconet' networks, which create a 'scatternet' network all together. Each piconet contains one functional unit, called master, and up to seven active units, called slaves. The transmitting power of slaves is at around 10 mW. The Bluetooth network works on non-license frequency band of 2.4 GHz containing 79 channels. The network can suffer from interferences as the used frequency band is non-licensed and e.g. the WLAN networks can work within the same frequency. The first modulation used for Bluetooth technology was GFSK (Gaussian Frequency Shift Keying), nowadays it can use either the  $\pi/4$ -DQPSK or 8DPSK. The duplex communication transmission rate can be up to 3 Mbps. [19]

The topology of the BLE technology is pictured in Fig.2.10. The blue part follows the typical star topology and the green part represents the mesh configuration providing a clue of how these topologies cooperate within the network. The cooperation of these two topologies enables extension of the system range. [19]

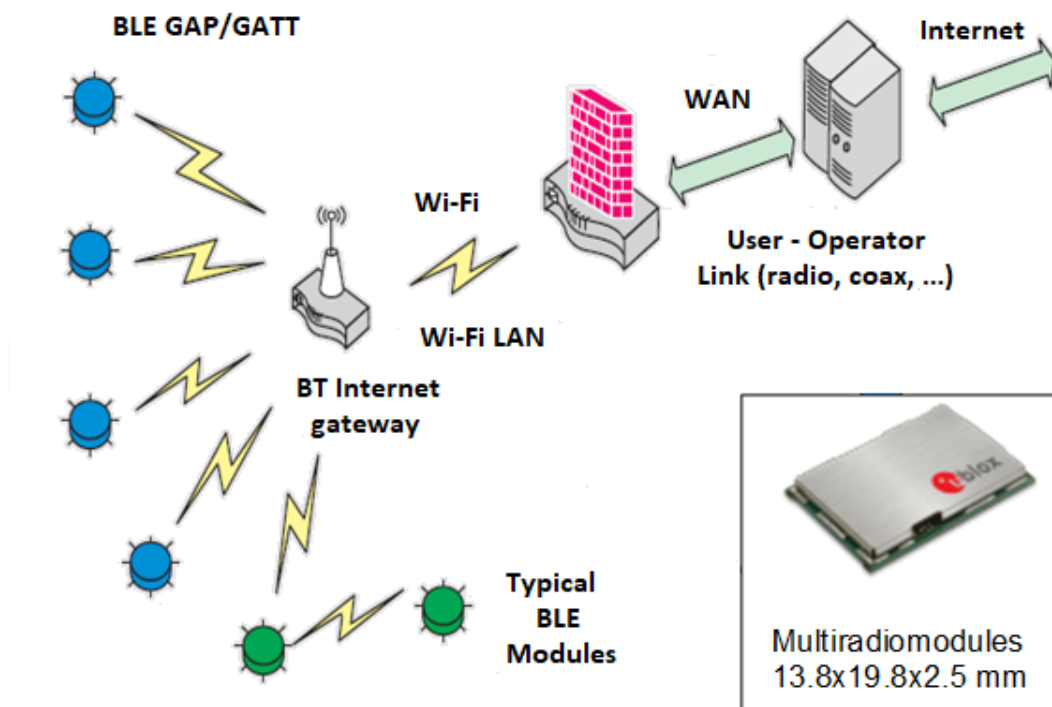


FIGURE 2.10: The topology of Bluetooth Low Energy network for IoT[19]

## 2.3 Summary

In this section, the networks supporting the IoT technologies have been introduced divided into the LP-WANs and Short-range Area Networks. Each of these networks benefits from their low power consumption but each of them suits better to different applications.

The SigFox network covers almost the entire area of the Czech Republic (and also Europe) and benefits from the low-cost of the final devices and wide signal outreach (upto 50 km in rural and 3-5 km in urban areas). On the other hand, there is a limited amount of messages that can be sent per day. It is 140 12-byte messages per day downlink and only 4 messages per day uplink. The SigFox network is most commonly used in weather stations, water consumption monitoring systems, etc. [17]

The LoRa network provides bi-directional data transmission with no day limit with an adaptable transmission rate of 300 bps (bit per second) to 50 kbps. Unlike SigFox, the data transmitted over LoRa network are saved in network provider's (CRA's) servers (SigFox saves all data transmitted over the networks on servers in France). LoRa also provides the option of building a private network available only in a defined area, which can be very useful for the IoT integration in private company networks. Therefore, the LoRa network is most commonly integrated in private companies to transmit data between IoT devices within a defined private network. [17]

The NB-IoT network is an extension of the mobile providers' services using LTE where the software of LTE base stations must be adapted to integrate NB-IoT. Each device within this network must include the communication module with SIM (Subscriber Identity Module) card for data transmission. The transmission rate is much higher than in case of SigFox or LoRa and the NB-IoT can be theoretically (when needed software is included) used anywhere, where the LTE network is. Moreover, the main advantage of licensed networks is that they can ensure a reliable system service without interference and they can perform real-time bi-directional monitoring. The NB-IoT network would be the most suitable for our remote animals' vital signs monitoring system as it provides bi-directional communication, no limitations of the number of messages and it covers the Czech Republic almost perfectly. [19, 17]

The short-range area networks usually transmit data from human wearable devices, such as smart watches, to the user's smartphone where their short range is not a problem.

The system designed in this thesis could implement both, the LP-WAN and short-range networks, to switch from the LP-WAN (NB-IoT) to short-range network (BLE) to save power when the animal's owner is near and also to retain the communication of the wearable system with the owner's smartphone even though the owner is not anywhere near the animal.

## Chapter 3

# Thesis objectives

The thesis objective was to formulate a study about the animals' vital signs monitoring and, based on the knowledge achieved in Chapter 1, design a wearable device which could monitor the main animals' vital signs remotely without disturbing the animal at all.

In chapter 1.1, principles of laboratory vital signs measurement have been introduced. The above described devices' principles give us an idea about each technology and about its usability for the IoT wearable devices. Moreover, chapter 1.2 provides a different approaches for the remote animal health monitoring of two non-commercial systems and their efficiency. From chapter 1 it becomes obvious that some of the laboratory health monitoring systems are more suitable for the animal remote health observation than others.

The main aim of this thesis is to help the animal owners or handlers to provide their pets the correct welfare and also to supply them with information about their pets' health and safety even during the owner's absence. Therefore, various experiments for the vital signs monitoring and data transmission will be performed to provide the best solution for the remote animal health management. Ideally, the most often laboratory monitored vital signs, such as the temperature and heart rate, should be observed remotely by a smart animal collar.

First of all, the ECG system introduced by Rita Brugarolas and her team will be purposed as a part of the final device design. After that, the heart rate remote monitoring device based on the principle of pulse oximetry will be suggested and the achieved data will be discussed. Thirdly, the animal's motion activity monitoring will be executed in the following experiment where the accelerometer module will be programmed to count the animal's steps as a pedometer. Fourthly, the surface body temperature's dependency on the core body temperature during activities of various intensities will be clarified by the experimental measurement. Finally, the data transmission over a LP-WAN network will be introduced with the data visualisation to the end user over cloud.

# Chapter 4

## System Design

Based on the studies introduced in 1.2.1 and 1.2.2 and the principles of systems for veterinary animal health monitoring described in chapter 1.1, the final device for remote animals' vital functions monitoring can be designed with respect to its reliability, cost, ease of use, animal non-disturbance and low power consumption.

Due to the matter of fact, that animal kinds differ one from another significantly from the body built, body thermoregulation, fur/feather density, etc., point of view, the system will be designed mainly with the respect of mammals' body built, especially dogs. The designed system will take into account dog's body and physiological properties and the separate designed subsystems will be experimentally tested on two dogs.

The designed system will be composed of several separate monitoring devices (sensors) and optimal wireless network for data transmission. Hence, every part of the designed system will be tested independently of others to conclude whether the suggested system for the specific vital function monitoring(or data transmission or other) is relevant in wireless animal health management or not.

### 4.1 Components

The system components have been designed based on the studies described above and on the assumptions supported by the principles of above described sensors functionalities and physiological processes of animals. The demands on the low power consumption and high reliability of all system components must be considered.

The design will contain ECG monitoring system supported by the study of [1], the pulse oximetry sensor, the body surface and ambient temperatures monitoring sensors and the accelerometer for the animal's activity tracking. The LP-WAN network will be designed for data transmission.

#### 4.1.1 ECG Electrode System

The ECG electrode system design is based on the study of [1], where six copper alloy spring-loaded gold-coated pins by Mill-Max Mfg. are soldered on a mini print-circuit-board (PCB) to create a comb-shaped array. Each pin is of 1.07 mm diameter, 8 mm maximum height and 0.51  $\mu\text{m}$  gold plating. The operating range of this pin electrodes is from  $-55^{\circ}\text{C}$  to  $+125^{\circ}\text{C}$ . [24]

Moreover, the animal-skin impedance can be reduced by the electrodes coating by conductive polymer layer. For more information about this system refer to chapter 5.1.

The one pin electrode is pictured below on Fig.4.1. Fig.4.1b presents the AD8232 Heart Rate Monitor device for pin electrodes signal processing described below. For the comb-shaped array of pin electrodes, refer to Fig.5.1.



(A) Spring-loaded gold-coated pin electrode [24]



(B) Heart Rate Monitor AD8232 [25]

FIGURE 4.1: Components for ECG monitoring

The ECG system requires at least three electrodes for its correct functionality. These electrodes are then connected to an Analog Devices AD8232 Heart Rate Monitor Front End which can extract, amplify and filter the small biopotential signals, such as ECG signal, despite the noise created by motion or others. AD8232 enables to set the cut-off frequencies of both the two-pole high pass filter for the motion artefacts elimination and the three-pole low-pass filter for additional noise removal. [25]

TABLE 4.1: Heart Rate Monitor Front End AD8232 [25]

Parameter	Min - Typ - Max	Units
Power-Supply Voltage	2.0 to 3.5	V
Supply Current	170	$\mu\text{A}$
Electrode Configuration	2 or 3	-
Signal Gain	100	-
Half cell potential	up to $\pm 300$	mV
Common-mode rejection ratio	80	dB

#### 4.1.2 Pulse Oximetry System

The pulse oximetry devices for animal heart rate monitoring usually comprise of two LED diodes of RED and IR wavelengths and a photodetector for each of them. The data are processed from both photodetectors where one wavelength is absorbed better during the systolic heart beat phase and the second wavelength during the diastolic phase. The pulse oximetry principle is described in more detail in chapter 1.1.1.

Therefore, for this system design the high-sensitivity pulse oximetry module MAX30102 was selected. The module is pictured in Fig.4.2 below.

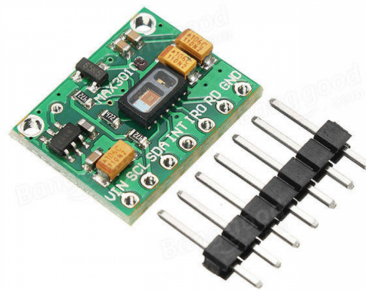


FIGURE 4.2: Pulse oximetry MAX30102 module [26]

The module communicates through a standard I<sup>2</sup>C interface and it provides a software module shut-down solution with ultra-low shut-down current ( $0.7\mu\text{A}$ ) while the power rails remain powered. The MAX30102 module is suitable for the IoT wearable device due to its ultra-low power operation. The module specifics are plotted in table 4.2 below. [26]

TABLE 4.2: High-Sensitivity Pulse Oximeter MAX30102 [26]

Parameter	Min - Typ - Max	Units
Power-Supply Voltage	1.7 1.8 2.0	V
Supply Current	600 1200	$\mu\text{A}$
ADC Resolution	18	bits
ADC Clock Frequency	10.32 10.48 10.64	MHz
IR LED Wavelength	870 880 900	nm
IR LED Forward Voltage	1.4	V
IR LED Radiant Power	6.5	mV
RED LED Wavelength	650 660 670	nm
RED LED Forward Voltage	2.1	V
RED LED Radiant Power	9.8	mV
Photodetector Sensitivity Range	600 900	nm
Operating Temperature Range	-40 to +85	$^{\circ}\text{C}$

### 4.1.3 Temperature Monitoring System

The surface and the ambient temperatures monitoring will be performed with the usage of two DS18B20 digital temperature sensors from DALLAS. These sensors are calibrated to the temperature accuracy of  $\pm 0.5^{\circ}\text{C}$  within the temperature range of  $-10^{\circ}\text{C}$  to  $+85^{\circ}\text{C}$ . Due to its *1-wire* interface, more sensors can be wired in parallel to a single digital pin. The sensors are very small and light and they can be built into a waterproof package of a stainless steel tube of 6mm diameter. [15]

The pictures of the waterproof and TO92 package sensors are presented below in Fig. 4.3.



FIGURE 4.3: (Left) TO92 sensor package, (Right) Waterproof sensor package [15]

More information about the digital temperature sensor is described in table 4.3 below.

TABLE 4.3: Temperature Sensor DS18B20 [15]

Parameter	Value	Units
Power-Supply Voltage	3.0 to 5.5	V
Temperature Range	-55 to +125	°C
Accuracy (-10 to 85 °C)	±0.5	°C
Programmable Resolution	9 to 12	bits
Active Current Consumption	1 to 1.5	mA
Query Time	< 750	ms

#### 4.1.4 Motion Activity Tracker

The MPU6050 six-axis (accelerometer + gyroscope) MEMS motion tracking device was designed by InvenSense for the low power and low cost applications of high-performances. The device is integrated in 4x4x0.9 mm QFN package and it combines a 3-axis gyroscope and a 3-axis accelerometer with the Digital Motion Processor (DMP) which processes the implemented InvenSense's MotionFusion firmware. Due to the integrated MotionFusion data output, the intensive motion processing computation requirements are offloaded by the DMP from the system processor and hence, the polling frequency of the motion sensor output is minimized. Above that, the internal DMP supports low-power pedometer functionality when the system processor sleeps while the DMP maintains the step counting. Moreover, the digitally programmable low-pass filters can be set by the user for signal high-frequency noise filtering. [27]

The device also offers an auxiliary master I<sup>2</sup>C bus to access additional external sensors, e.g. magnetometers, which enables the device to gather a set of data from all sensors without system's processor intervention and then provide a complete 9-axis Motion-Fusion output. The I<sup>2</sup>C serial communication interface with the system processor is supported by the MPU6050. [27]

The picture of the MPU6050 InvenSense device is shown in Fig.4.4.



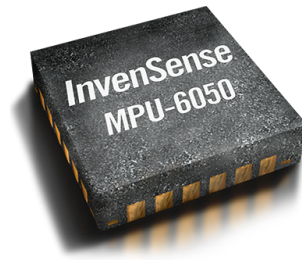


FIGURE 4.4: MPU6050 MEMS module [27]

The accelerometer full-scale range of  $\pm 2g$ ,  $\pm 4g$ ,  $\pm 8g$  or  $\pm 16g$  is programmable by the user as well as the full-scale range of gyroscope ( $\pm 250$ ,  $\pm 500$ ,  $\pm 1000$ ,  $\pm 2000$   $^{\circ}/\text{sec}$ ). The device also includes the 1024 FIFO buffer for further power consumption reduction when the sensor data can be read in bursts and then a low-power mode can be entered when MPU collects more data. Moreover, the  $V_{logic}$  reference pin is provided by the device to set the logic levels of its I<sup>2</sup>C interfaces. All axes of both accelerometer and gyroscopes outputs are processed by 16-bit ADCs. [27]

The more detailed information about the MPU6050 device is introduced in table 4.4.

TABLE 4.4: InvenSense MPU6050 Six-Axis MEMS MotionTracker [27]

Parameter	Value	Units
<b>Supply Voltage (<math>V_{DD}</math>)</b>	2.375 to 3.46	V
$V_{logic}$ Reference	$1.8 \pm 5\%$ or $V_{DD}$	V
<b>Accelerometer Full-Scale Range</b>	$\pm 2, \pm 4, \pm 8, \pm 16$	g
<b>Gyroscope Full-Scale range</b>	$\pm 250, \pm 500, \pm 1000, \pm 2000$	$^{\circ}/\text{sec}$
<b>Gyroscope Operating Current</b>	3.6	mA
<b>Gyroscope Standby Current</b>	5	$\mu\text{A}$
<b>Accelerometer Operating Current</b>	500	$\mu\text{A}$
<b>6-axis DMP Operating Current</b>	3.9	mA

#### 4.1.5 Data Processing and Transmission

The microcontroller must fulfil the demands of the IoT technologies, which require a low power consumption, but they also must provide all the interfaces needed for sensors introduced above and the support for the data transmission network(s). The ESP32 system on a chip microcontroller is very suitable for the designed system's purposes for its low power consumption and low cost. It also integrates Wi-Fi and dual-mode Bluetooth for either classic or low energy data transmission, which could be used for communication of the designed system with the animal's owner's smartphone when they are near to each other.

Nevertheless, the most suitable network for the causes of this study is the LP-WAN NB-IoT network which works within the licensed frequency spectrum and hence, ensures no data collisions, and which can send unlimited amount of data per day. Some IoT development kits, such as the Pycom Fipy or Arduino MKR NB1500 boards, include the modem for the LTE NB-IoT low-power data transmission with microcontroller of low power consumption. The Fipy development board from Pycom contains, besides others, both the ESP32 microcontroller and the NB-IoT network modem. For more information about the Fipy development board refer to Fig.5.22. The Arduino MKR

NB1500 development board runs on SAMD21 Cortex-M0 microchip and the NB-IoT and LTE Cat M1 wireless network connectivity is supported by the U-blox SARA-R410M-02B Module. Both development boards can be powered either over the USB port or by a Li-Po (Lithium-Polymer) single cell batteries which are very suitable for wearable electronics for their lightness. [28]

Unfortunately, the NB-IoT network required components are not available to be tested in this thesis. Therefore, some basic data will be transmitted over the SigFox network and the example of the data visualization in E-mail and Cloud will be introduced in chapter 5.5. Although, the SigFox network has limited data size for transmission and quantity of messages transmitted per day, the animal critical states detected by the designed system's algorithm could be transmitted only. Otherwise, a normal animal health status would be considered.

## 4.2 Components Connection

The components' wiring remains the same regardless on the chosen microcontroller or development board, so the wiring will be introduced in a block diagram from the communication interfaces point of view.

There are four various systems for the remote animal's vital signs monitoring designed in this thesis.

**The ECG system** composed of three comb-shaped pin arrays and the heart rate monitor analogue front-end chip requires an analogue pin for the output signal, two digital pins for the Leads-off detection and the 3.3 V power supply for its correct functionality.

**The PPG system** based on the MAX30102 pulse oximeter module and **the pedometer system** which uses the MPU6050 MEMS accelerometer both benefit from their support of the I<sup>2</sup>C communication protocol where only two wires for the Serial Clock (SCL) and Serial Data (SDA) signals are necessary. This protocol also benefits from having one master for multiple slaves. Therefore, data from more slave devices can be transmitted over a single wire when they are correctly addressed. The data are bi-directionally transmitted between the master and the slaves bit-by-bit along a single SDA wire synchronized to the bits sampling by the SCL signal which is controlled by the master (Arduino MKR NB1500 here). [29]

**The PPG system's** must be powered from 1.7 to 2 V and **the pedometer device** requires from 2.375 to 3.46 V.

Finally, **the digital temperature sensors DS18B20** for the animal's body surface and the ambient temperatures monitoring require only one digital pin for both and the power supply from 3 to 5.5 V.

The block diagram below (Fig.4.5) pictures the connection of all sensors to the Arduino MKR NB1500 board.

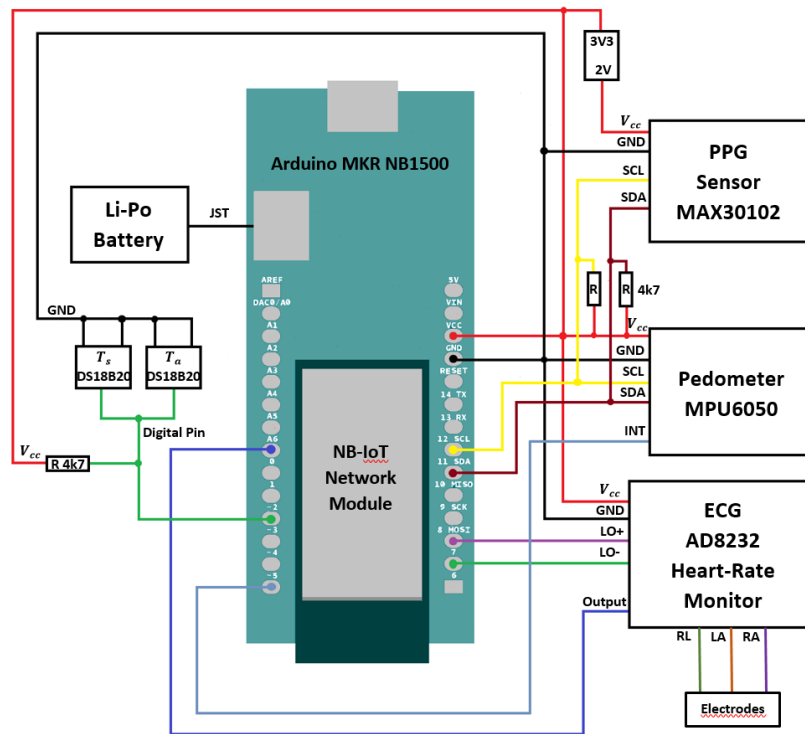


FIGURE 4.5: Block diagram of components wiring with the Arduino MKR NB1500 board

### 4.3 Sensor Deployment on Animal's Body

The most suitable locations of animals' bodies for the wireless vital sign observation are the chest and the neck where the collars or harnesses are usually worn by animals without disturbing them. Therefore, a typical dog or cat harness is very suitable for the overall system placement to get each sensor to work correctly. First of all, the harness ensures the sensors' placement to a fixed spot of the animal body. Secondly, the wiring from the central unit to every separate sensor can be sewn into the harness material and so isolated from the animal skin and ambient environment.

The chest belt of the harness can serve for the ECG electrodes and the central unit attachment to the animal's body.

The chest belt is very suitable for the ECG electrodes placement. The ECG measurement from chest leads is also integrated in the Holter monitoring device, although this device requires fur shaving for the correct electrodes adherence to the skin. Based on the study of [1], the ECG device for heart rate monitoring can be designed and the suggested placement of the electrodes to the animal's body can be followed.

Therefore, three gold-coated six-pin array electrodes coated with PEDOT:PSS can be attached to the chest belt of the harness. The chest belt electrodes' placement and the golden retriever wearing the chest belt of the overall system designed by Rita Brugarlos and her team are pictured in figure below.

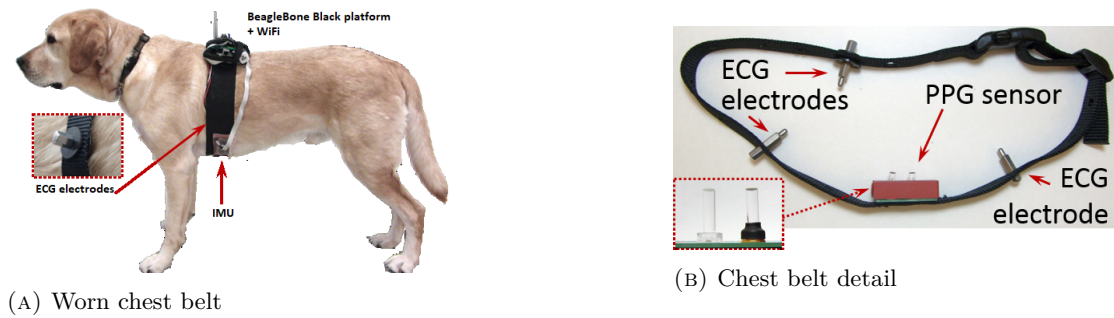


FIGURE 4.6: Overall ECG and PPG sensor placement [1]

On the other hand, placing the PPG sensor on a chest is not very suitable due to the rib bones which attenuate the incident light much more than the tissue and skin. In general, PPG sensors are placed on either very thin body parts, such as ears or tongues, when the absorptive mode is implemented, or on body parts, such as a wrist for humans, which are highly blood supplied and do not contain bones or much fat within the incident light path which would attenuate the light unexpectedly. Based on that knowledge, the chest belt seems out of options. Therefore, the PPG sensor will be wired from the central unit to the animal collar, 'a neck belt', and attached to the nether part of the neck where the carotid artery leads.

The surface temperature monitoring sensor will lead out from the bottom of the central unit box directly to the skin where it will be covered by the animal's fur from all sides. Animal fur serves as a thermal isolation so that the animal does not get cold and due to the matter of fact that the fur isolation is 'bi-directional', the fur should serve as a protection of the sensor not to get influenced by the ambient temperature.

Finally, the accelerometer for animal motion monitoring will be placed directly in the central unit box attached to the interface of the collar-chest connecting belt and the chest belt, so that the axes of the accelerometer remain in the same position corresponding to the animal's body.

Therefore, the central unit box, attached to the interface of the chest belt and the connecting belt, will contain the microcontroller board for sensors data processing, accelerometer, temperature sensor for ambient temperature monitoring and the transmission unit with antenna.

The components' placement on the canine body is pictured in Fig.4.7.

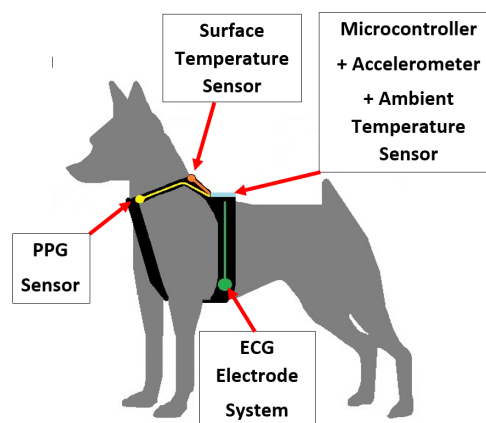


FIGURE 4.7: Components' placement on canine body

## Chapter 5

# Designed Systems' Functionality

As already declared, the above designed system validity will be clarified in several separate experiments.

First of all, the ECG heart rate monitoring system designed by Rita Brugarolas and her team will be described. Secondly, the PPG heart rate monitoring on the carotid artery will be performed and the obtained data will be analysed. After that, the pedometer for the animal motion activity will be introduced using the accelerometer device and its capability of authentic step counting will be clarified from several experiments of various dogs. Fourthly, the static spot surface temperature dependency on the animal core temperature will be determined. Finally, the SigFox network data transmission will be tested to present a representative of the LP-WAN networks (chapter 2.1) which are more suitable for the animal remote health monitoring than the short-range networks described above (chapter 2.2).

Unfortunately, the NB-IoT network which seems to be the most suitable for our case became out of options due to the SIM cards non-affordability. Therefore, the SigFox network has been chosen as LP-WANs' representative.

### 5.1 ECG Monitoring System

The wearable ECG monitoring system for dogs has been already introduced in chapter 1.2.1. In this part of the thesis, the ECG system designed by [1] will be described with respect to its efficiency and reliability.

#### 5.1.1 In-Vitro Experimental Analyses

The authors studied various electrode shapes and materials to enhance the electrode-tissue coupling and to reduce the electrode-tissue impedance caused by the animal fur. Therefore, two types of electrodes for wireless recording ECG signals were observed: millimeter thick stainless steel pointed cycle electrodes (RFA-529) and array of one millimeter thick spring-loaded gold-coated pins (Mill-Max Mfg.) soldered to a mini printed-circuit-board (PCB). The impact of the number of thinner pin electrodes compared to the thicker stainless steel electrodes to the overall impedance and the enhancement of the pin penetration through the animal fur has been studied by the authors. Moreover, to decrease the impedance even more, they coated the gold-coated pins with PEDOT:PSS conductive polymer. The impedance dependency of various number of pins and of the PEDOT:PSS conductive polymer electrode coating are plotted in Fig.1.5 in chapter 1.2.1.

The process of coating is described in [1] in detail. The observed electrodes are pictured below in Fig.5.1. In the figure, the comb-shaped array electrodes with ten and four gold spring-loaded pins, where one of them is coated with the PEDOT:PSS conductive polymer and the second one is not, are compared to the stainless steel electrode from the size point of view.

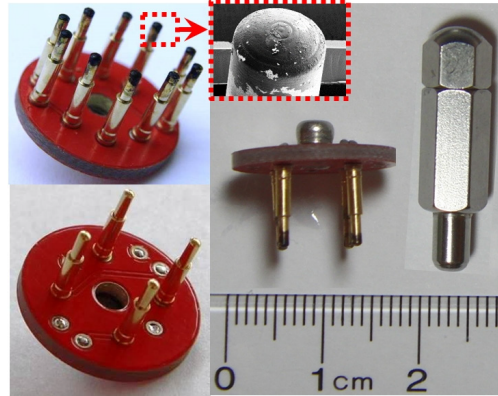


FIGURE 5.1: (Left) Pin array of PEDOT:PSS coated (upper corner) and uncoated (lower corner) electrodes, (Right) relative sizes of both types of observed electrodes [1]

The impedance responses of pointed style stainless steel electrode, the array of four spring-loaded PEDOT:PSS coated pins and the traditional ECG patch electrode attached to a shaved spot of the animal's body are represented in the plot below in Fig.5.2. They performed the same measurement for all electrode types both with and without applied electrolyte gel which decreases the interface impedance even more. From the plot below it is clear that when the electrolyte gel is applied to the stainless steel and pin electrodes in a hairy region, the impedance is even smaller for the low frequencies than in case of the patch electrodes attached to a shaved spot during clinical monitoring.

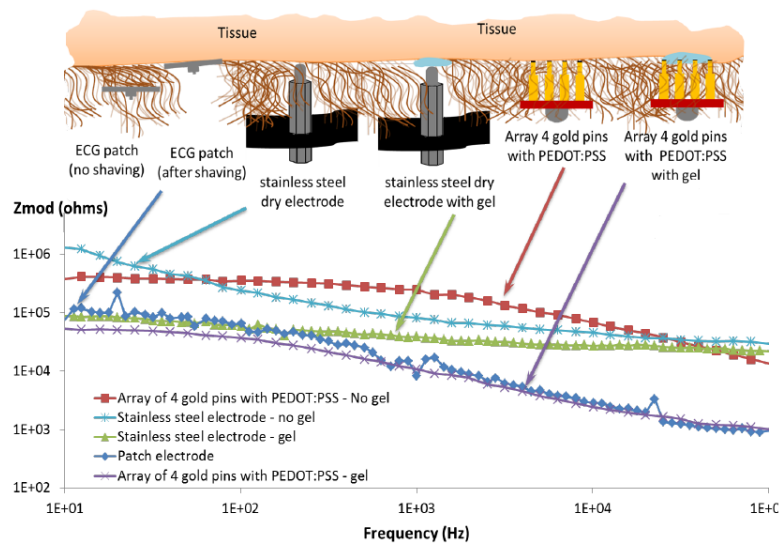


FIGURE 5.2: *In-vitro* experiment - patch/stainless steel/gold spring-loaded four pin array [1]

The tissue-electrode impedance can be equivalently described as a series combination of resistance ( $R_{el}$ ) and in parallel connected resistance ( $R_{ct}$ ) and capacitance ( $C_{el}$ ). The  $R_{el}$  represents the thermal noise caused by the cumulative effect of tissue, electrodes and some additional resistance caused by wiring and connectors.  $C_{el}$  refers to the electrode capacitance originated at the electrode-tissue interface and the capacitance rising results to more significant signal distortion. The  $R_{ct}$  refers to the ability of the electrode-tissue interface to transfer a charge from one to another. The four-pin gold-coated array electrode determined lower  $R_{el}$  and  $C_{el}$  than the stainless steel electrode when no electrolyte gel was incorporated.

### 5.1.2 In-Vivo Experimental Analyses

Based on the *in vitro* analyses the most suitable electrodes for the ECG wearable heart rate monitoring system have been selected and the *in vivo* analyses have been performed.

The *in vivo* analyses referred to the system accuracy by comparing it with the Holter monitoring device as reference and determining the system reliability by recording recruited dogs during activities of various intensities.

The authors performed the ECG measurement with five leads of the Holter device and the ECG surface electrodes with electrolyte gel attached to shaved body areas to serve as reference and three comb-shaped six-pin electrodes of the designed system covered by electrolyte gel placed to a chest-strap behind the animal's front legs (refer to Fig. 4.6) in a hairy area. They performed 12 minute long measurement when both Holter monitoring electrodes and the examined six pin comb-shape array electrodes covered by PEDOT:PSS coating were attached to the dog's thorax. The heart beats were recorded when the dog performed various activities, divided to static (resting) and dynamic (walking). The measured results of the R-R duration (interval between two heart beats) are plotted bellow. From Fig.5.3 it is clear that when the animal is resting, the designed system reports very similar results as the Holter device and only 0.34% of the Holter device detected beats were missed by the designed system. On the contrary, during the 10-minute long walking phase of the experiment the results slightly differ, when 5.4% of the beats detected by Holter device were missed by the pin array electrode system.

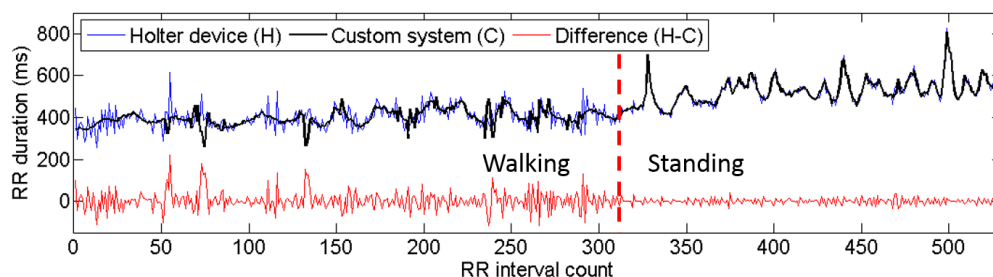


FIGURE 5.3: In-vivo experiment [1]

Furthermore, the system's evaluation during activities of various intensities has been performed. The integral modules of accelerometer (IMA) were utilized for the activity intensity detection.

In this experiment, they computed the ratio, called statistical indices sensitivity (SE), of the correctly detected true positive beats (TP) over the sum of TP and the undetected beats and the ratio, called specificity (SP), of TP over the sum of TP and falsely detected

beats. The IMA was used for the high, or low, intensity of each activity detection and its result is plotted as the green line in Fig.5.4. The R-R interval between the following QRS signals has been observed and if the interval exceeded the specified range, undetected beat has been indicated. Contrariwise, when the R-R interval was shorter than specified range, the falsely detected beat was indicated.

The authors concerned more about the correct heart rate (HR) and heart rate variability(HRV), through the R-R interval, detection than about the full PQRST waveform observation. Therefore, in order to remove motion artefacts, they designed the narrow-band filter for further signal processing, which caused some signal distortion and only the QRS waveform has been observed by the system. The ECG recorded signal from the designed system of three arrays of six gold spring-loaded pins with respect to the activity intensities monitored by the IMA unit is plotted below in Fig.5.4.

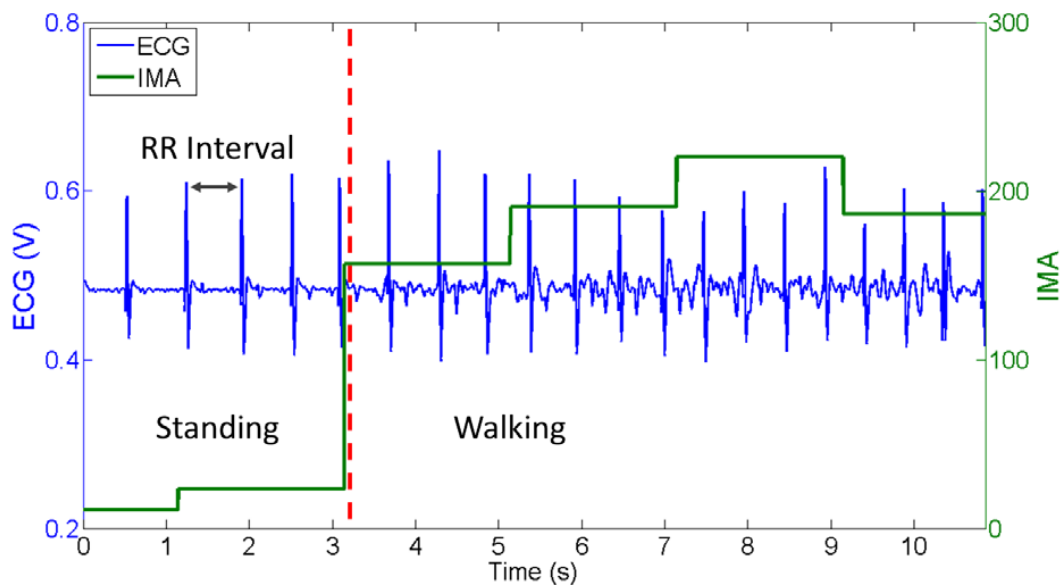


FIGURE 5.4: R-R interval monitoring [1]

### 5.1.3 Final System Design

The final system consists of three 6-pin gold- and PEDOT:PSS-coated spring-loaded electrodes placed on the dog's thorax which are wired to the front-end analogue chip AD8232 for the analogue signal processing.

The obtained results refer to the system's good performance and its usability for the remote heart rate monitoring of animals. This system, with some adaptations, could be suitable for heart rate monitoring of also other animals than dogs only.

Nevertheless, this robust system for animal heart rate monitoring serves as an example of the matter of fact that any wearable health monitoring system is suitable mainly for training purposes or, in this case, for learning more about the animal's emotional reactions to specific stimulus. Any wearable device for daily usage cannot supplant the medical examinations provided by a vet (or doctor). In case of this system design it is obvious, for example, from the signal processing by the narrow band filter which removes the unwanted motion artefacts on the expenses of the desired ECG PQRST waveform disruption.



## 5.2 PPG Monitoring System

This experimental project is based on the system built by Ing. Luděk Dudáček who tests the pulse oximetry method of human heart rate monitoring. The principles of both human and animal heart rate monitoring based on the pulse oximetry method are the same, although the animal fur attenuates the light significantly.

As already declared, the PPG heart rate monitors are already frequently used in the laboratory environments, but the laboratory pulse oximeters are usually clipped on tongues or ears of the animals when they are sedated to achieve the most relevant results as they are based on the pulse oximetry's absorption mode. These two spots are out of options for wearable devices. Based on the study of [1], the impact of the animal fur is significant. Nevertheless, the most suitable animal body part, suggested in chapter 4, will be measured.

### 5.2.1 Hardware

The heart rate monitoring device includes the MAX30102 pulse oximeter module for the heart rate monitoring and the STM32F100 microcontroller for data processing. The communication between them is performed via the serial bus of  $I^2C$ .

The block diagram is pictured in Fig.5.5.



FIGURE 5.5: Block diagram of the experimental system

The pulse oximeter module includes two internal LED diodes, two photodetectors and low-noise electronics with ambient light rejection. The LEDs work within the RED and IR (infrared) wavelengths. The IR diode operates from 870 nm up to 900 nm and the RED diode works from 650 nm up to 670 nm. The module was set to the  $SpO_2$  and heart rate measuring mode where both LED diodes were activated with transmission speed of 50 samples per second (sps). The MAX30102 can be controlled through software registers and the 32 - FIFO (First IN - First OUT) shift register is integrated for managing the obtained digital data. It can hold up to 32 data samples depending on the number of active LED channels, which is configurable. As already declared, both channel for both LEDs were activated in this system. While each sample consists of two data channels and there are 3-byte data per channel, 6-byte data for each sample are transmitted. Hence, 192 data bytes can be stored in the FIFO register.[26]

The basic block diagram of the integrated pulse oximeter's circuit is plotted in Fig. 5.6.

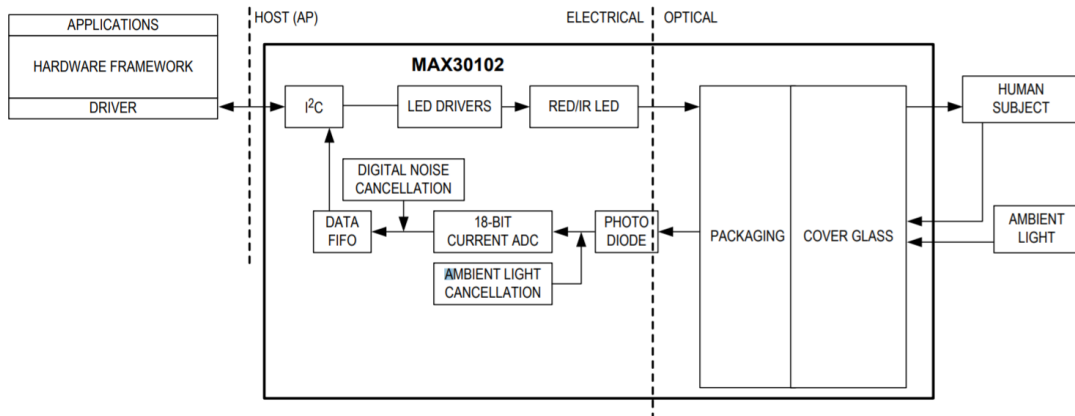


FIGURE 5.6: The block diagram of MAX30102 [26]

The data from the pulse oximeter were then transmitted every half second to the microcontroller 128 - buffer memory. After that, the data were processed by two FIR (Finite Impulse Response) filters where one of them was low-pass filter and the second one was high-pass filter for data from both the RED and IF LEDs. The UART (Universal Asynchronous Receiver Transmitter) communication interface was utilized for the data transmission from the microcontroller to the PC. On the PC screen, the data were displayed and saved as a .csv file, where the original raw output of the pulse oximeter, the DC and AC components of the signal were present as functions of time for both RED and IR LED diodes. The DC component of the measured signal is an output of the low-pass filter and the output of the high-pass filter introduces the AC component of the measured signal.

The block diagram of the data processing is in Fig.5.7.

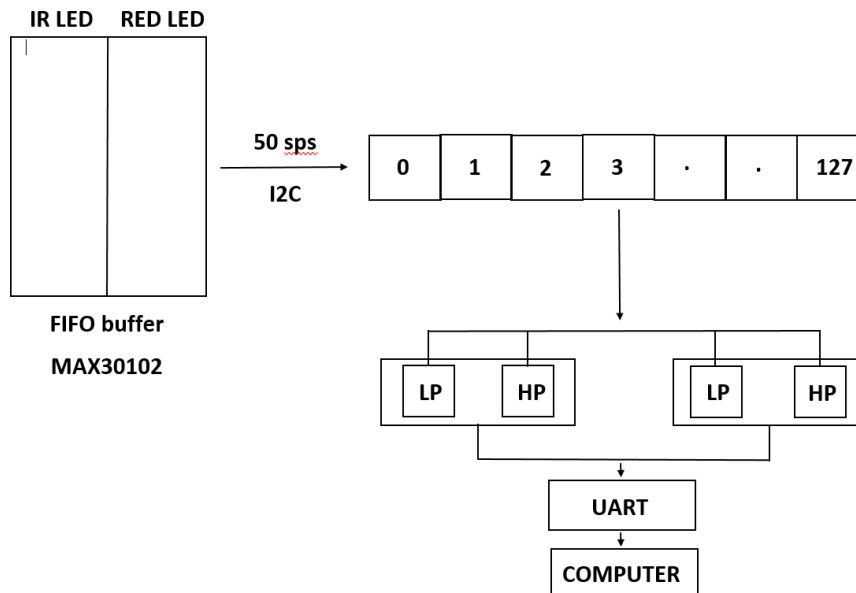


FIGURE 5.7: The data processing from pulse oximeter

### 5.2.2 Experiment Set-Up

Two dogs of mix breed, each of them with different density of hair layers, were used as test subjects for the non-invasive heart rate monitoring with the usage of the above described device.

TABLE 5.1: Information about experiment participants

N.	Name	Age	Hair type	Weight
Dog 1	Andy	2 year old	Mid-long/Soft/Dark	11 kg
Dog 2	Štafik	5 year old	Short/Raw/Light	9 kg

Beside the spot, front neck, designed in 4, the data were scanned also on their earlobe and groins, the inner part of their left back leg, to ensure that the designed spot is the most suitable for sure. These three spots represent very convenient parts of the animal body for heart rate measurement. The earlobe, as already declared, can be monitored in the laboratory environment to obtain the animal's heart functionality and the animal groin serves as an example of a spot where there is a bit lower density of hair layers and which is strongly blood supplied. The front neck neck is very practical for wearable devices, because it does not disturb the animal and due to the matter of fact that the carotid artery leads there.

As table 5.1 reports, the first dog has black mid-long hair of higher density, yet its hair is softer, while the second one's hair's density is lower and his hair is shorter, light and raw.

Both dogs were sitting as still as possible during each measurement and their hair was not shaved, but the device was attached to the skin as tight as possible without any necessary hairs disturbing the measurement.

The measurement results are presented in the section below.

### 5.2.3 Measured Data

The canine heart beat can differ significantly according to the dog's size and breed (information from MVDr. Kateřina Melicharová). While the big breeds' heart rate can be very slow, even around 60 bpm at rest, in case of the small dogs the common heart rate is significantly increased (even up to 140 bpm at rest).

The heart rate of the first dog was measured by a reference pulse oximeter device to determine range of expected heart rate for the mid-sized dogs. The veterinary Capnograph Monitor provided by the Veterinary High School in Plasy was utilized for this purpose. The  $SpO_2$  percentage value and the heart rate/ pulse rate (PR) of the animal was measured.

During the measurement the dog's heart rate was from 118 to 121 bpm and the  $SpO_2$  was 98% (refer to Fig.5.8). Both values are reasonable for this specific dog's size. The heart rate was measured also during the animal's sleep and after a physical activity. Therefore, the heart rate range of this dog was appointed to be from 80 to 145 bpm.



FIGURE 5.8: Pulse Rate and  $SpO_2$  of the first dog measured by Capnograph Monitor

Finally, the first dog's heart rate was measured by above designed PPG system. Obtained signals from both photodetectors and their frequency analyses limited by the frequency range of canine heart rate determined by the reference measurement are plotted below in Fig.5.9.

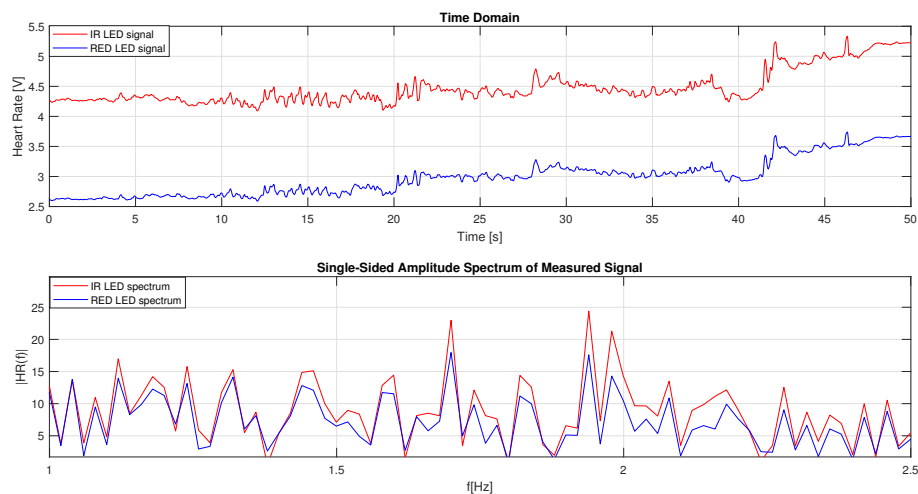


FIGURE 5.9: The measured signals from the pulse oximeter - first dog, front part of neck

Following analyses have been performed to distinguish the desired signal from the noise.

#### 5.2.4 Measured Data Analyses

The FFT (Fast-Fourier Transform) analyses of the 50-second long measured signal (plotted in Fig.5.9) has been performed for 10 second sections of the signal separately in this section. The sampling frequency was set to 50 Hz during the measurement and the FFT analyse is plotted within the frequency range stated from the canine heart rate range to be approximately from 1Hz (1.33Hz for the mid-sized dog) to 2.5Hz (2.417Hz).

The window-based bandpass FIR filter was designed in MATLAB environment to eliminate the frequencies which do not correspond to the dog's heart rate range (1.33 - 2.417Hz). The range was determined by a reference measurement explained above. The Hamming window was integrated by the FIR filter to eliminated the frequencies out of the specified range. Nevertheless, such a narrow window requires very high filter order to attenuate unwanted frequencies of, at least, 3dB. Unfortunately, the higher the filter order is, the longer is the filter's delay. Therefore, the filter order, finally set to 56, was designed with respect to the filter delay and the cut-off frequencies attenuation. The

filter attenuation of the cut-off frequencies is -2.4 dB, but the heart rate range of all canine breeds can be from 60 bpm to 140 bpm at rest, which means that after physical activity the upper boarder even increases. The attenuation at the frequency of 1Hz which correspond to 60 bpm is more than -6dB as well as the frequency of 2.5 Hz (150 bpm).

The designed filter could be used for a real-time PPG data processing in a final device manufactured with respect to the designed system. The filtered signal can be plotted as a function of time and when it exceeds a dynamic threshold counted from a floating average of several following samples, the heart beat would be detected.

The 10 second interval of the measured raw signal from the IR photodetector interpolated by the filtered signal and the filtered signal spectrum is plotted below in Fig.5.10. The peak frequency of the filtered signal refers to 2.096 Hz which corresponds to heart rate of 125.76 bpm.

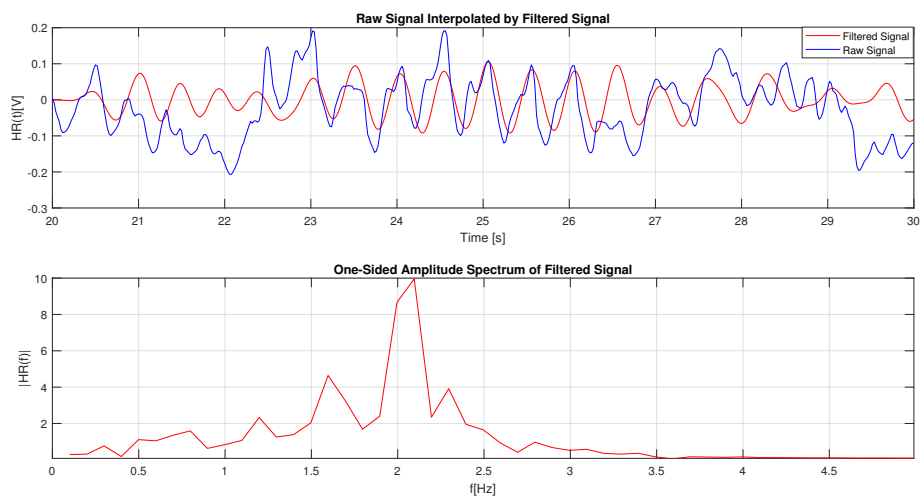


FIGURE 5.10: Time and frequency spectrum [10,20]s interval

The 56-order FIR filter magnitude responses is pictured in Fig.5.11 in logarithmic and in linear scale.

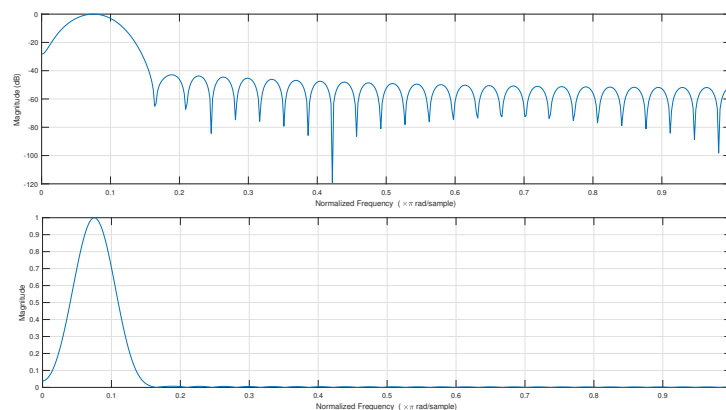


FIGURE 5.11: 56-order FIR filter magnitude responses

The FFT analyses of all 5 intervals performed separately are pictured below in Fig.5.12. It is obvious that the first interval, during which the PPG sensor was not attached to the animal's skin almost all the time, does not contain almost no desired signal. The second interval, already pictured above also with the filtered signal in time domain, has the dominant frequency of 2.096 Hz same as the third interval. Fourth and fifth interval detected lower frequencies with lower amplitude than the second interval, where the heart beat was clearly visible from the time domain already.

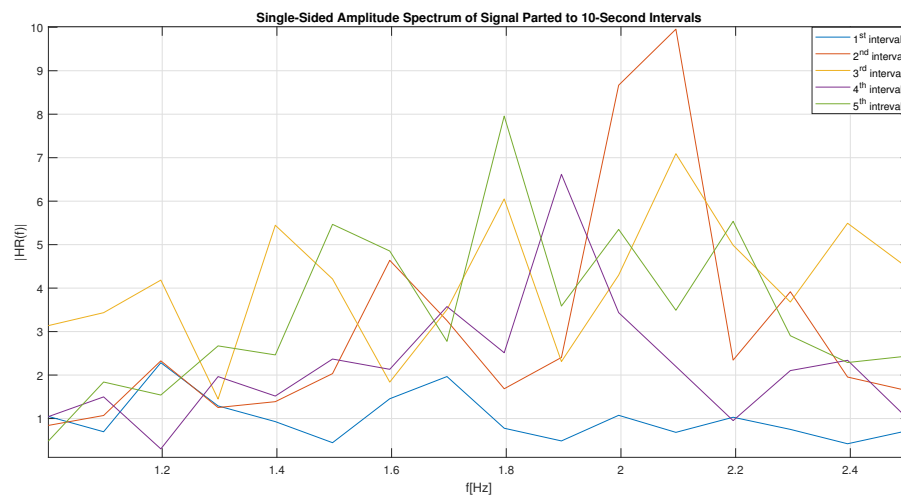


FIGURE 5.12: Single-sided spectrum of all five intervals

## 5.3 Pedometer for Motion Activity

The following experiment ensures the usability of the pedometer, the step counter, in the animal health management for the activity monitoring of animals.

The pedometer was created with the usage of the MPU6050 module, which includes, as described above in chapter 4.1, the 3-axis accelerometer, 3-axis gyroscope and the DMP. The program was written in C++ programming language on the Arduino IDE platform and the data were processed by Arduino Nano board with the ATmega328P microcontroller.

### 5.3.1 Model Description

The acceleration is usually the main parameter used for the motion detection. When the nature of walking is considered, it usually works the same for all mammals. Pedometers analyse the user's steps based on the matter of fact that at least one axis has relatively significant periodic acceleration variations when the user walks or runs. Contrariwise, the acceleration in remaining two axes changes considerably from time to time, but not repeatedly with a specific time period.

If we consider the accelerometer placement as described in chapter 4.3, that is the animal's back, the motion axes will remain the same with respect to the animal's body all the time. In this case, the periodic acceleration is within the  $z$  axis when the specified MPU6050 module placement on the animal's body is respected.

The most challenging part of the pedometer algorithm is to set up the most suitable acceleration threshold, which above the footstep can be detected. When the same pedometer was tested on humans, the periodical acceleration was much more obvious and the peak-to-peak deflection was more significant than when tested on dogs which is caused by the human height. Considering all sizes of dogs, the threshold and the peak-to-peak deflection will also vary from size to size, it will depend on the animal's height, legs length, etc.. Nevertheless, if we want to declare the threshold successfully, the raw data from the accelerometer must be processed firstly.

At first, the raw accelerometer data in 2' complement format were transferred to the  $g$  acceleration units. The low acceleration mode of the accelerometer is set in this project, because no rapid velocity variation are expected, or possible, by the running animals. Hence, the accelerometer full-scale was left as default to  $\pm 2g$  which is enough for the pedometer application. Therefore, the raw data from all three axes were divided by 16384 LSB/g (Least Significant Bit/gravity acceleration unit).

After that, the high-frequency noise has been reduced in the obtained data by adaptive averaging of every three newest samples. The unwanted high-frequency noise has been filtered by this part of the algorithm. Its principle is pictured in Fig.5.13.

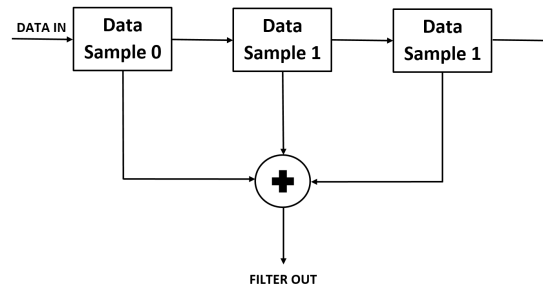


FIGURE 5.13: High-frequency noise filtering

Moreover, to ensure that any additional noise will not interrupt the correct step counting, the acceleration difference between each two following samples must remain above specific precision. Therefore, after the *averageZ* has been calculated, its absolute division with the previous valid value (*validZ*) was compared to the appointed acceleration precision. The following equation must be fulfilled to write the current *averageZ* value to the *validZ* variable and to the *FiterDataBuffer[i]* for further processing.

$$\text{abs}(\text{averageZ} - \text{validZ}) < \text{precision}$$

The *precision* is set to 0.005 g which refers to the acceleration of  $4.9 \text{ cm/s}^2$ . When the minimal step length of dogs is considered to be 10 cm, then such a small acceleration is not relevant for the step monitoring of dog, as it would refer to acceleration of only half a step per second for the smallest dogs. Therefore, such data can be filtered. Using the precision and the floating average calculation for data processing a conscious error is inserted to the pedometer accuracy, but it also filters the noise. The error of half missed step per second for the smallest dog breeds is then considered.

The difference between the raw data from the accelerometer transferred to *g* units and the filtered data of a short time sequence of samples is plotted below in Fig.5.14.

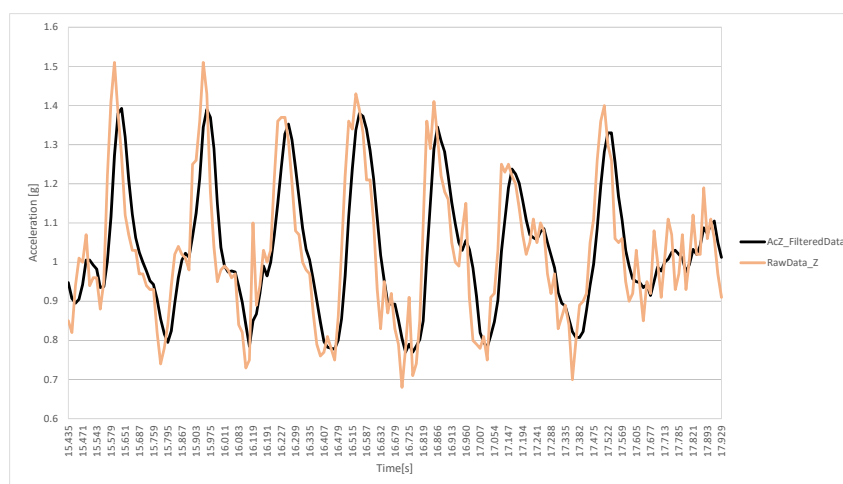


FIGURE 5.14: Filter data to accelerometer raw data comparison



### 5.3.2 Results Evaluation

As already described, the algorithm is adapted to count the steps of a dog where one step is considered when the animal moves forward one front and one back leg. The algorithm counting reliability was tested on two dogs introduced in Tab.5.1. The threshold for the step counting has been set manually in the algorithm to 1.2g after several experiments which confirmed it as the most suitable for the most accurate step detection. The experimental measurements detected that lowering the threshold level below 1.2g causes detection of fake steps caused by unfiltered noise. Contrariwise, if the threshold was set above 1.2g the more steps were not detected. Therefore, the threshold level of 1.2g seems to be the limit threshold for the most accurate step detection. The threshold settings was based on compromise of the noise filtering and the pedometer accuracy for slowest steps detection.

Finally, the dogs have been repeatedly (5 times each of them) monitored by the pedometer when walking and then the actually taken steps were compared with the steps counted by the pedometer algorithm. The results of these experiment are presented below in Tab.5.2 and Tab.5.3. The first column of the table refers to the experiment number. The **Pedometer** column introduces the quantity of steps counted by the pedometer algorithm. The **Threshold Exceeds** column statements come from post-analyses where the measured data in Z-axis were plotted and the steps were counted from the quantity of threshold exceeds of the filtered signal. The step counter considers every threshold exceed only once until it falls below the threshold again to count a step. The last column contains the quantity of steps actually taken by the animal. It was counted by eye by two different people at once to ensure, that the result number is correct.

TABLE 5.2: Five experiments on pedometer - the first dog

N.	Pedometer	Threshold Exceeds	Actual Steps
1.	34	34	36
2.	55	55	59
3.	26	26	25
4.	42	42	45
5.	19	19	19

TABLE 5.3: Five experiments on pedometer - the second dog

N.	Pedometer	Threshold	Actual Steps
1.	22	22	21
2.	45	45	39
3.	30	30	27
4.	11	11	10
5.	54	54	51

From the plot below, Fig.5.16, it is clear that when the dog gallops, runs fast, the peak-to-peak deflection is more significant and hence, the pedometer step detection is more accurate. On the other hand, when the dog moves slowly, the z-axis acceleration is very close to the threshold level or even below and a step does not have to be detected.

Examples of measured data represented in a plot are pictured below in Fig.5.16 and Fig.5.15 containing the raw data, the filtered data, the threshold and the steps counted

by the algorithm. From the plots it is clear that the raw data acceleration is usually a bit higher than in case of the filtered data. In some cases the raw acceleration exceeds the threshold, but the value of the filtered data does not, which would lead to a missed step detection, if the specific acceleration actually referred to a valid step. The first plot introduces an error step detection within the second and fourth step, where the filtered average data, calculated from following three data samples, exceed the threshold and fall back twice within a very short period of time. It is caused by high frequency noise which was not filtered enough.

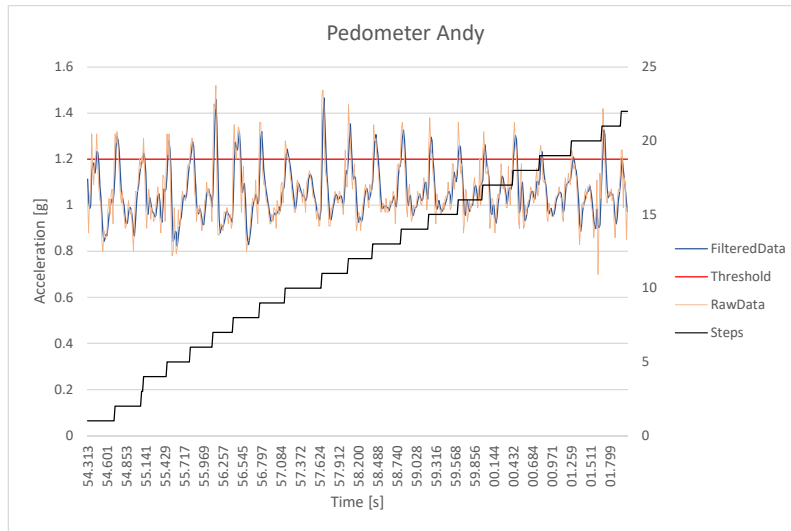


FIGURE 5.15: Pedometer data - the first dog

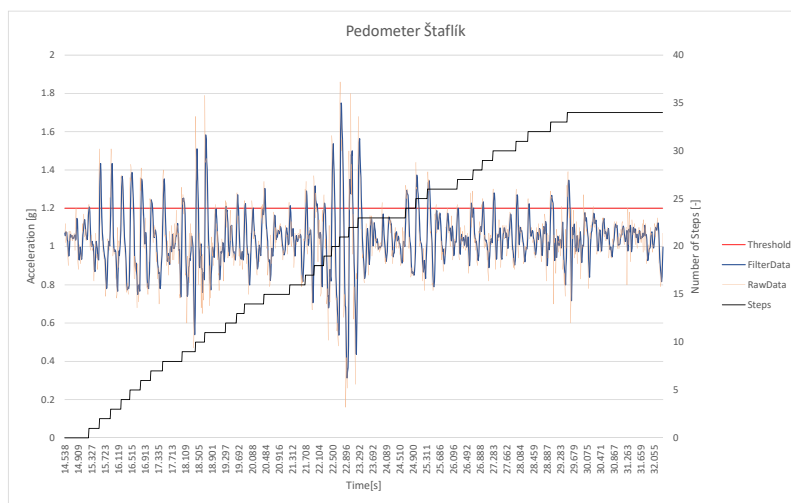


FIGURE 5.16: Pedometer data - the second dog

## 5.4 Surface - Core Temperatures' Dependency

This experiment observed the correlation between the animal's core temperature and the animal's surface skin temperature with respect to the ambient temperature and the animal's motion activity.

### 5.4.1 Wiring

Two digital sensors DS18B20 described in chapter 4.1, which benefit from the *1-wire* interface, were connected in parallel to the Arduino Nano digital pin D7. The first sensor monitored the ambient temperature and the second sensor was placed under the animal's fur to a fixed body spot. The entire device was wired as pictured below (Fig.5.17) and attached to the animal's harness on its back as described in chapter 4.2.

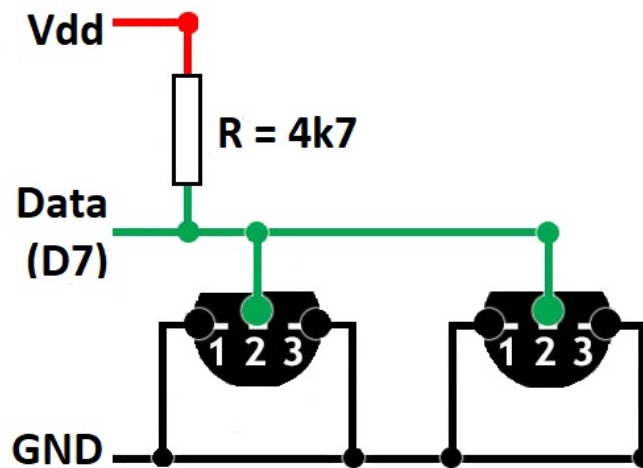


FIGURE 5.17: Wiring of temperature sensors to Arduino

### 5.4.2 Experiment Set-up

The experiment contained of 2-minute resting period at the beginning, six minutes of dynamic running (a ball chasing) and four minute of resting at the end. The second dog's surface and core temperature responses were observed in this experiment.

To retain the sensor-skin contact during all dog's activities as tense as possible, the sensor wires were sewn into the harness neck belt. It is easier to eliminate the fur from below the belt on the neck and to keep it so even during dynamic activities, such as jumping and shaking, than from the dog's back where the fur is usually smoother.

The core temperature was monitored during the experiment to discover the relation between core and surface temperatures. The Sanitas SFT 75 Multi-function thermometer was used for this purpose. The ear measurement accuracy of this thermometer is declared to be  $\pm 0.2^{\circ}\text{C}$  and it takes only few seconds to estimate the temperature.

### 5.4.3 Measurement Results

During first two minutes the animal laid still to stable the surface temperature and it settled down to  $34.4 \pm 0.1^{\circ}\text{C}$ . During the first resting period of the experiment, the

core temperature was measured by the Sanitas SFT 75 thermometer four times to ensure it does not change. The core temperature was confirmed to be  $38.2^{\circ}\text{C}$  by all four measurements during the first resting period.

During the 6 minutes of running interval, the core temperature was measured every 1.5 minute and the surface temperature was observed continuously every 15 seconds by transmitting the data over Bluetooth Low Energy module to the smartphone. The various measuring frequencies are caused by the matter of fact that if the core temperature would be measured too often, the animal would not get so much into the activity due to the too frequent breaks. Contrariwise, the surface temperature could have been monitored by the wearable device and the more frequent readings introduced quite an interesting view to the surface temperature alternation during various activities.

Therefore, one core temperature measured by SANITAS thermometer was considered relevant for 6 following surface temperature measurements (1.5 minute). Both the core and the surface temperatures were slightly increasing during the animal's physical activity.

Finally, a few minutes of resting followed to observe how temperatures alter when the animal rests after the physical activity. It took approximately four minutes for both temperatures to lower back to the almost default state which was measured before the activity.

The dependency of the core and surface temperatures is pictured in the plot below (Fig.5.18) which represents the measured data by the SANITAS thermometer and by DS18B20 digital temperature sensor attached to the animal's skin. Some values measured by the DS20B18 temperature sensors sometimes slightly fell below the previous value while the next value was higher again without any obvious reasons. Such values were considered as a fault data and they were replaced by the previous value.

The plot below declares that both the core and the surface temperatures vary depending on the physical activity of the animal. The core temperature increases within the first 1.5 minute for  $0.2^{\circ}\text{C}$  and then with the following measurement up to  $38.7^{\circ}\text{C}$  where it stables for 3 more minutes of activity and 1.5 minute of resting. Then it lowers to  $38.4^{\circ}\text{C}$  during 4 minutes of resting.

On the other hand, the surface temperature varies more and even when the core temperature does not alter, the surface temperature still rises during the activity. Of course, it can be caused by frequencies in which each measurement has been executed.

Nevertheless, the surface temperature dependency on the core temperature is obvious and more measurements in various environments and various canine breeds should be executed to specify a model of these temperatures dependencies within various ambient temperatures.

During the entire measurement, the ambient temperature was  $18.3 \pm 2^{\circ}\text{C}$ .

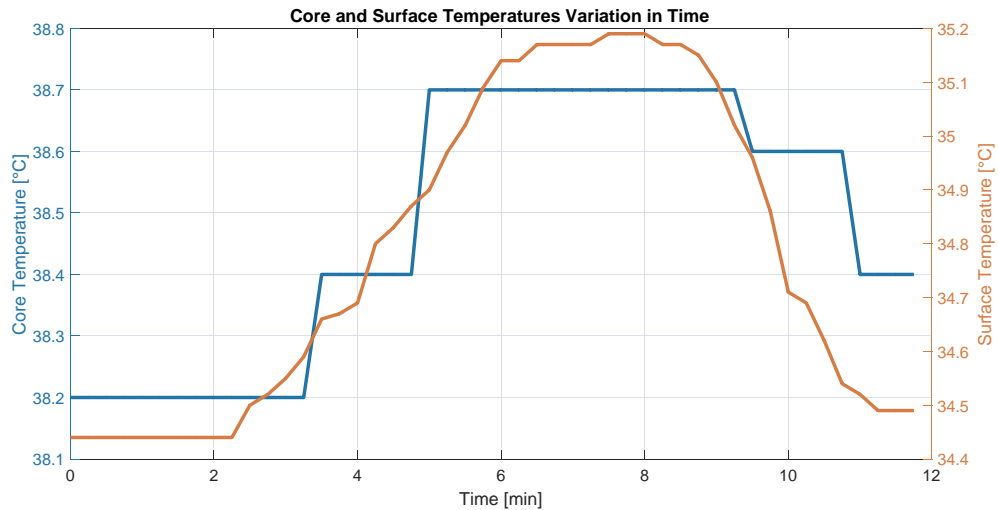


FIGURE 5.18: Core and Surface skin variation in time during various activities

The lowest and the highest core temperatures measured by the SANITAS digital thermometer during the experiment are pictured below in Fig.5.19.



(A) Measured core temperature before physical activity



(B) Measured core temperature after physical activity

FIGURE 5.19: Core temperature measurement by SANITAS thermometer

#### 5.4.4 Equivalent Thermal Model

The equivalent thermal model considering the designed system, canine body and the ambient temperature will be designed. It is based on the matter of fact that every tangible body loses part of the supplied power when it is transformed to thermal energy and so the body's temperature rises. The temperature rise depends on the supplied power, body's weight and material, etc. The non-isolated body transfers its heat to the ambient environment, which can be the air, radiator, etc., and the thermal energy transfer rises with the temperature difference of the ambient environment and the body. Its thermal resistance can be specified based on the supplied power and the temperature difference which is expressed by the equation below.

The  $R_{\vartheta}$  refers to the thermal resistance,  $\vartheta_a$  is the ambient temperature,  $\vartheta_m$  is the material temperature and  $P$  it the supplied power.[30]

$$R_{\vartheta} = \frac{\vartheta_a - \vartheta_m}{P} = \frac{\Delta\vartheta}{P}$$

Even though it is clear from the Fig.5.18 that the surface temperature depends on the core temperature of the animal's body, the thermal model representing the thermal losses of the surface temperature monitoring system is designed. The core and the measured surface temperature by the system differ due to the thermal resistances caused by animal

tissue and the junction between the skin and the temperature sensor which is caused by the imperfect adherence of the sensor to the skin and by the sensor's package.

The equivalent model could serve for further measurements when the system would be tested in various conditions, such as lower/higher ambient temperature, etc.

In this case, the core temperature ( $\vartheta_{core}$ ) was 38.2°C. The skin temperature ( $\vartheta_{skin}$ ) obtained from the measurement by the DS18B20 sensor which was held adhered to the animal's skin was 34.62°C. The skin temperature measured by the designed system ( $\vartheta_{measured}$ ) was 34.44°C. The  $R_{\vartheta tissue}$  refers to the thermal resistance of all layers of animal's tissue, the  $R_{\vartheta junction}$  represents the thermal resistance of the imperfect adherence of the temperature sensor to the animal's skin and the  $R_{\vartheta sen}$  is the thermal resistance of the temperature sensor itself.

The ambient temperature was 18.1°C.

The equivalent thermal model is pictured on the Fig.5.20.

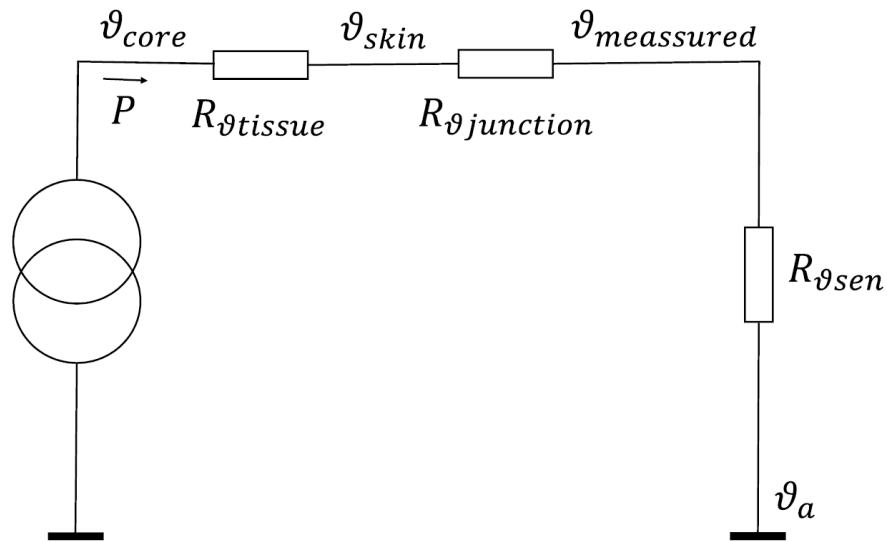


FIGURE 5.20: Equivalent thermal model of the entire system

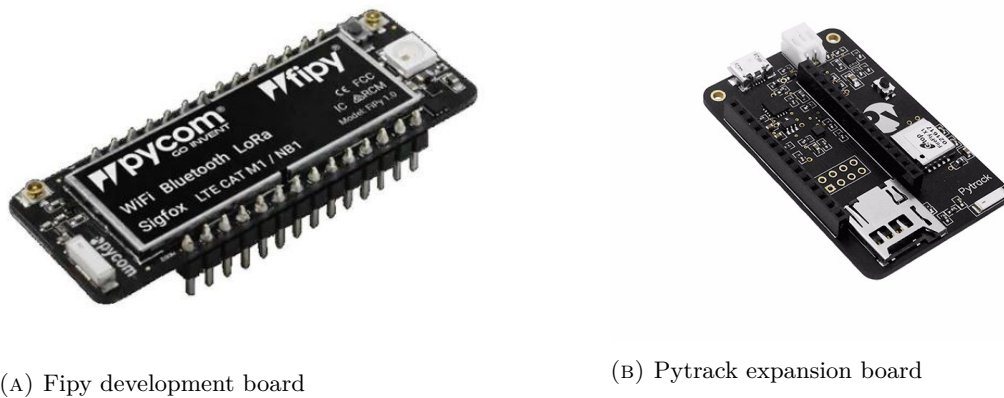
## 5.5 SigFox Data Transmission

The last experiment is focused on the data transmission by using the representative of the LP-WAN IoT supportive network. The experiment is performed on the IoT devices provided by the Pycom company. This company specializes on the expansion of IoT supportive hardware and software for the prime development of various IoT projects. The Pycom boards are very useful for the prime device development for its low energy consumption and great variety of options of the required project solution. On the other hand, Pycom boards are not so common and hence, the user service base, such as the quantity of libraries for external modules and sensors, is not so extended as in case of the Arduino family and the Pycom developers are still improving some software bugs and non-functionalities. Hence, the Pycom devices and the provided services enhance and change very often.

The data transmission via the SigFox network is tested as the representative of the LP-WAN network family. As already declared, the SigFox network has been chosen due to several reasons. The best choice for our goal would be the NB-IoT network for its light antenna, best coverage and non-limited bi-directional data transmission, but due to the cost of the necessary SIM cards which were offered for 3000 CZK for a start-up package of 20 SIM cards, this network became out of options for this project. Hence, the SigFox data transmission is implemented in the last experiment for the SigFox network's good area coverage (in the entire Europe) and low cost and due to the matter of fact, that LoRaWAN network is more usual in case of more extensive projects where lots of IoT devices are connected within the network, e.g. within a company private network. On the other hand, SigFox is very common of usage for data transmission in individual projects such as this one.

### 5.5.1 Hardware

This project includes two boards provided by Pycom. First of them is the development board called Fipy, which provides 5 different IoT supportive networks all described in chapter ???. The second one is the Pycom extension board, called Pytrack, which provides the microUSB serial port for code/firmware uploading to the both expansion and development boards and the JST connector for the Li-Ion/Li-Pol battery device power supply (the battery can be even charged from the board when it is powered via the microUSB connector). Moreover, this specific expansion board includes the GPS/GLONASS module for location tracking, the microSD card slot and the 3-axis 12-bit accelerometer. The biggest disadvantage of this board is the matter of fact that it provides only ten external I/O (input/output) pins, which are mostly useless due to the firmware which does not support the external sensor connection to the I/O pins.



(A) Fipy development board

(B) Pytrack expansion board

FIGURE 5.21: Pictures of Pycom devices from [www.pycom.io](http://www.pycom.io)

Furthermore, an external antenna for the SigFox data transmission has to be attached to the Fipy board so that the board does not get damaged during the transmission.

Moreover, the external analogue low voltage temperature sensor TMP36 has been included to measure the ambient temperature. The information provided by the manufacture about the Pytrack's external IO header are quite unclear. From the first point of view, it seems that the IO header provides 10 pins, where 3 of them supply power, 1 serves as GND and the rest of them are analogue input/output pins for external sensors and modules wiring. Even though the first pin really stands for the ground and the second, third and fourth pins provide the power to external sensors, the rest analogue pins are not correctly wired to the Fipy pinout or supported by the firmware. The EXT-I01 external pin, which should lead to P9 (ADC included on that pin) of the Fipy development board, has been tested as an example and no data from the external sensor has been obtained. The official Pycom documentation does not explain the external IO header usage in much more details, but the Pycom official forum ([www.forum.pycom.io](http://www.forum.pycom.io)) provided an explanation of this non-functionality as it is supported by the Pycom employees. The ESP32 module which is included in all Pycom modules enables to map the I<sup>2</sup>C interface to any of these external pins, but unfortunately, non of the external IO header's pins is wired to ADC1 converter on the Fipy side and the ADC2 converter is not supported by the Pycom firmware at all. Hence, the external IO header cannot be used for the external analogue modules connection. Even though the information comes from a public Pycom forum and it is not official, it seems as a possible explanation of the non-functionality.

For the detailed pinouts of both Fipy and Pytrack boards refer to Fig.5.22 and Fig.5.23 below.



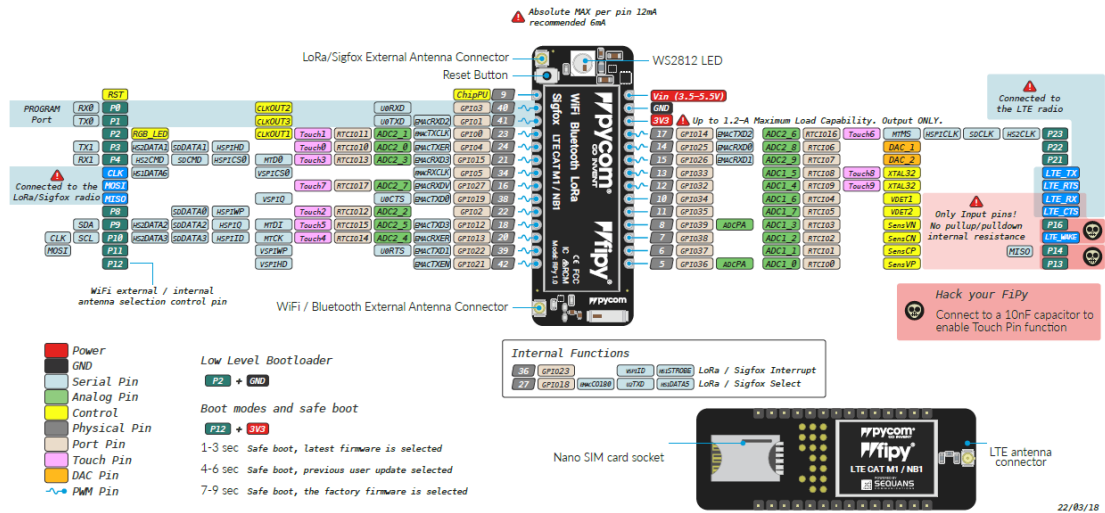


FIGURE 5.22: Pinout diagram of development board Fipy

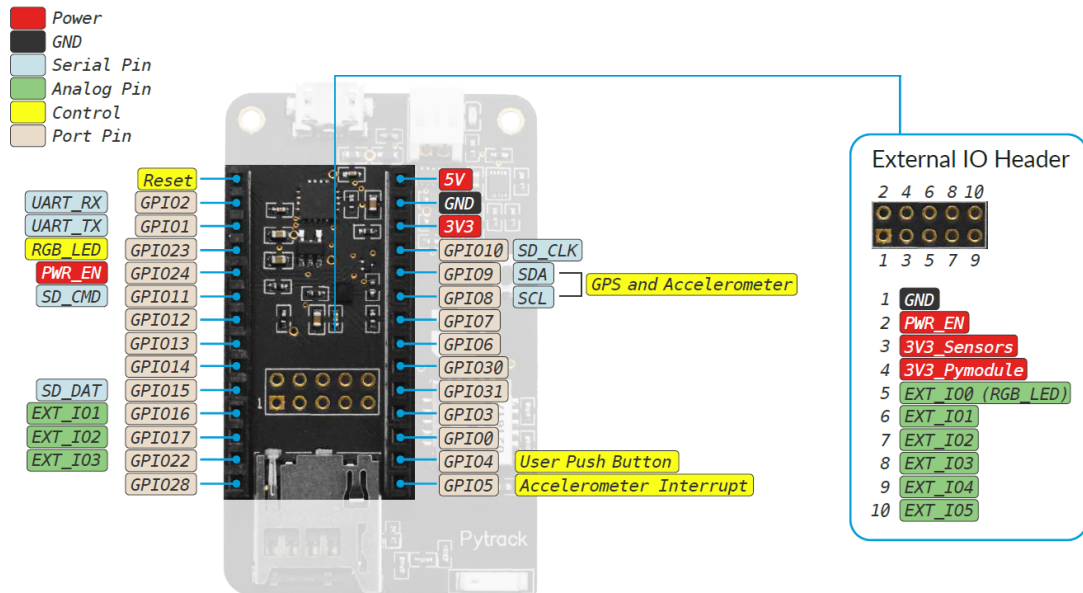


FIGURE 5.23: Pinout diagram of expansion board Pytrack

Hence, another approach has been implemented. The TMP36 temperature sensor can be directly connected to any analogue pin of the Fipy development board if it includes the ADC1 converter and if it is not used by any embedded module in Pytrack for communication with Fipy. For our cause, the P16 has been chosen and the data from the external temperature sensor has been processed via the Fipy board. Even though, this solution is not really elegant as the temperature sensor pin has to be soldered directly to the bottom side of the board and it only proves that the Pycom board serves better for development purposes only, it provides a possible solution for the external modules integration to this project.

The final wiring of the final device is pictured in Fig. 5.24

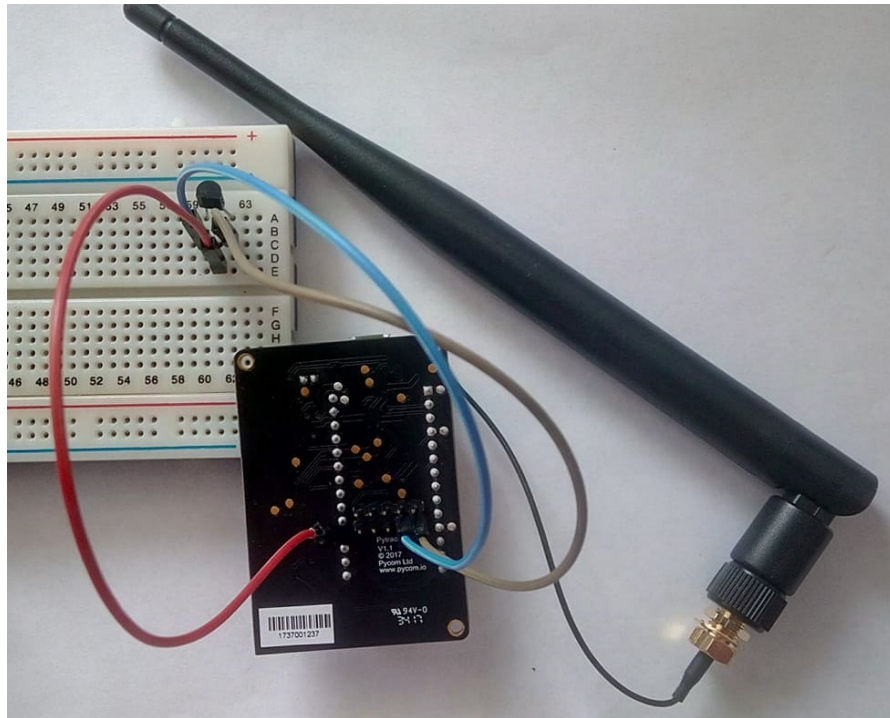


FIGURE 5.24: Components' wiring

### 5.5.2 Software Environment

The Pycom devices' based project with the SigFox network for data transmitting has been handled, from the software point of view, in several levels of the data processing and transmitting.

As the devices' firmware update process is not considered as this thesis objective and there are quite detailed instructions on the official Pycom website how to update the firmware, it will not be described and the introduction of the programming editor will follow.

The **Atom editor** with the Pymakr plugin serves for programming the system with the desired functions. The Pymakr is an Atom package which enables to communicate with the Pycom board via the build in command line REPL (Read-Evaluate-Print Loop). The Atom editor supports many programming languages but this project was written in MicroPython because it is recommended by Pycom. Although, the MicroPython includes only limited support of the standard Pycom libraries, it benefits from its adaptation for running on microcontrollers or in any constrained environment.

A part of the Atom code in MicroPython programming language including the REPL line is plotted in Fig.5.25. For the entire code with the necessary comments refer to the attached documents SigFox-GPS and SigFox-Temp.

```

77     #if coord are read, perform commands below
78     if not coord == (None, None):
79
80         lat, lng = coord
81         mVolts = apin.voltage()
82         deC = 25.0/750.0 * mVolts # 750 mV refers to 25 degC
83         location(lat, lng, deC)
84
85         # wait for specific time (2 minutes)
86
87         time.sleep(120)
88

```

```

Connected ✓ No project
RTC Set from NTP to UTC: (1970, 1, 1, 0, 1, 53, 47825, None)
Adjusted from UTC to EST timezone (1970, 1, 1, 2, 1, 53, 3, 1)

Connect to SigFox network
(49.73255, 13.36199) - (1970, 1, 1, 0, 1, 54, 298832, None) - 2540288
The latitude and longitude coordinates are: 49.73255 13.36199
The ambient temperature is: 20.0
(49.73255, 13.36199) - (1970, 1, 1, 0, 4, 16, 756604, None) - 2540720
The latitude and longitude coordinates are: 49.73255 13.36199
The ambient temperature is: 18.6

```

FIGURE 5.25: Part of the code written in Atom for Pycom device

### 5.5.3 User Interface

After the data are sent over the SigFox network, they display on the **SigFox backend**, where the user can either watch them hexadecimally encoded or transfer them via set callbacks to other user interfaces, such as to the email or to various clouds. In this project, the data are transferred to both email and the ThingSpeak cloud.

The example of one loop of sent data visualized in the SigFox backend website is pictured in Fig.5.26

Time	Data / Decoding	LQI	Callbacks	Location
2019-05-03 16:35:31	31382e3636363637			
2019-05-03 16:35:21	343937333234313333363139			

FIGURE 5.26: Data from SigFox backend encoded in hexadecimal data type

The data can be decoded in any hexadecimal to string converter and the result of the '343937333233313333363231' hexadecimal message would be '497324133619' where first 6 digits stand for latitude and last 6 digits stand for longitude. The second message would be decoded from '31382e3636363637' to 18.66667°C. After the first data were decoded it became obvious that without any additional data treatment, the results will not be easily readable if the user does not know which digits and which messages stand for what type of information.

Hence, the SigFox callbacks have been set to re-send the data to additional user interfaces and for additional processing. Due to the matter fact, that SigFox can transmit only 12 bytes of data payload in one message and that each GPS coordinate takes 6 bytes of data and the temperature 4 bytes of data, the coordinates and the temperature are sent every 15 minutes in two messages via separate experiments.

The **E-mail** custom callback setup in the SigFox backend website for GPS coordinates is pictured in Fig.5.27. The temperature callbacks have been set accordingly, only with the 'temp' variable instead of 'lat' and 'lng' and custom payload config is set to *temp::char:4*.

Callbacks

Type: DATA UPLINK

Channel: EMAIL

Send duplicate:

Custom payload config: lat::char:6 lng::char:6

Recipient: bulinovam@gmail.com

Multiple emails allowed separated by comma, semicolon or new line

Subject syntax: Subject with device {device}

Message syntax: Message containing time {time}, key1 {var1}, key2 {var2}...

Available variables: device, time, duplicate, snr, station, data, avgSnr, lat, lng, rssi, seqNumber

Custom variables: customData#lat, customData#lng

Subject: SigFox message

Latitude: {customData#lat}

Longitude: {customData#lng}

Message

FIGURE 5.27: Email callback for GPS coordinates

The coordinates are sent every 15 minutes to the user's e-mail displayed as follows:

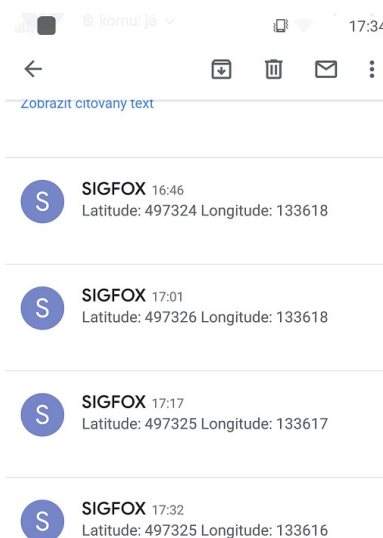


FIGURE 5.28: GPS coordinates sent to user's E-mail

The **ThingSpeak platform** custom callback setup for GPS coordinates is pictured in Fig.5.29.

Callbacks

Type

Channel

Send duplicate

Custom payload config  ?

URL syntax: <http://host/path?id={device}&time={time}&key1={var1}&key2={var2}...>  
 Available variables: device, time, duplicate, snr, station, data, avgSnr, lat, lng, rssi, seqNumber  
 Custom variables: customData#latitude, customData#longitude

Url pattern

Use HTTP Method

Send SNI  (Server Name Indication) for SSL/TLS connections

header	value

Content type

Body

```
lat: {customData#latitude}
lng: {customData#longitude}
```

FIGURE 5.29: ThingSpeak cloud callback

The ThingSpeak is an IoT platform for visualizing and archiving data from the desired device. Moreover, the additional data processing can be performed via inbuilt Matlab analysis.

First of all, the communication channel in ThingSpeak has been created for the GPS data visualization. When a channel is created, unique API keys are generated for the data writing and reading. This write API key serves as the identification of the data's desired destination for the SigFox Backend callback, where it is filled to the URL pattern with the variables that are supposed to be sent.

The channel settings are pictured in Fig.5.30. The first two fields contain the raw data from the device, while the third and fourth field refer to data processed with Matlab analyse.

## Channel Settings

Percentage complete 50%

Channel ID 770346

Name

Description

Field 1

Field 2

Field 3

Field 4

FIGURE 5.30: ThingSpeak channel settings for GPS

Afterwards, the data processing by Matlab analyse has been performed using the following code (Fig.5.31) which is set to be executed every time new data are inserted by the 'React' function.

```

1 % Enter your MATLAB Code below
2 readChannelID=[770346];
3 readAPIKey='SW741BDOP4ZW5PFH';
4 writeChannelID = [770346];
5 writeAPIKey='3TQIFCBX2X11SQY5';
6
7 format long
8
9 data = thingSpeakRead(readChannelID, 'ReadKey', readAPIKey, 'OutputFormat', 'table');
10 analyzedData = data;
11
12 analyzedData('Latitude') = data('latitude')/10000;
13 analyzedData('Longitude') = data('longitude')/10000;
14 analyzedData
15 thingSpeakWrite(writeChannelID, analyzedData, 'writeKey', writeAPIKey);

```

FIGURE 5.31: Matlab data processing

The output of the Matlab code for the GPS data is plotted in Fig.5.32.

Output				
analyzedData =				
1x5 table				
Timestamps	latitude	longitude	Latitude	Longitude
04-May-2019 15:01:53	497326	133618	49.7326	13.3618

FIGURE 5.32: Output from the Matlab code

Moreover, the obtained data can be also displayed graphically as a function of time, or dependent on each other, etc. The ThingSpeak platform enables us to process and watch the data in various ways according to the user's wishes.

The graphical interpretation of data obtained from the Pycom device are plotted in Fig.5.33. The temperature was displayed the same way as the GPS data and processed accordingly.

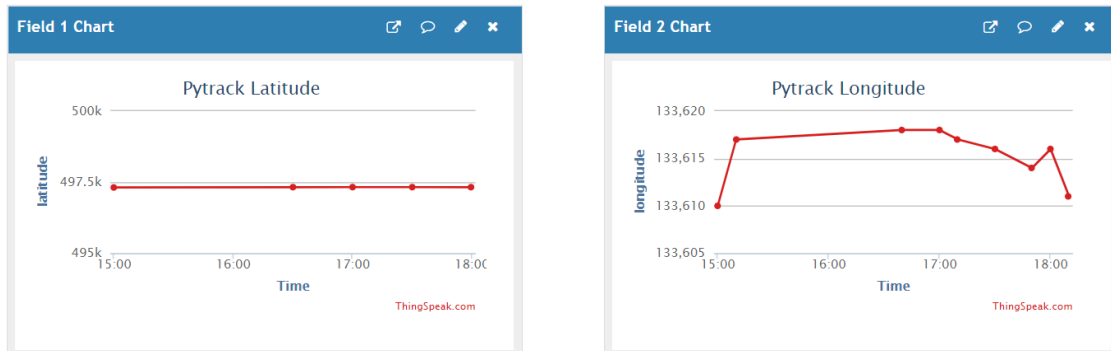


FIGURE 5.33: Graphical interpretation of the GPS data

## Chapter 6

# Discussion

The main thesis objective stated in chapter 3 contained the design of a wearable device for remote animals' health monitoring respecting the matter of fact that it should not disturb the animal, the output of the designed system should be reliable and it should be easily used by the animal's owner for daily purposes.

The health monitoring system designed in chapter 4 includes the ECG, PPG, temperature, activity tracking and data transmission subsystems where each of them is made to work separately to clarify its potential in animal remote health management and determine the subsystem's functionality.

### 6.1 Experiments Recapitulation

At first, the ECG heart rate monitoring system was suggested based on the study of Rita Brugarolas and her team [1]. After several various experiments they designed the system of three 6-pin gold-coated spring-loaded electrode arrays coated by the conductive polymer PEDOT:PSS. The data from the electrodes are processed by the front-end analogue chip AD8232.

Secondly, the PPG heart rate monitoring system performance was tested on two dogs. The subsystem contains of MAX30102 pulse oximeter device which monitors the blood volume changes in veins based on the principle of photoplethysmography.

Thirdly, the pedometer for animal's motion activity tracking was designed using the MPU6050 accelerometer+gyroscope device.

Fourthly, the surface temperature monitoring subsystem was integrated due to the impossibility of animal's core temperature monitoring. The correlation between the animal's core and surface temperatures has been observed.

Finally, the example of the system's data transmission over a LP-WAN network with the data visualization was introduced. Firstly, the designed system included the NB-IoT network for its most suitability for this project, but due to its unavailability at the time of the thesis work, the SigFox network data transmission has been integrated in the system design experiments as an example of IoT data transmission network.

### 6.2 Results Summary

The subsystems of the design device were made to work separately to test their functionality for the remote animal health management.



The study of the overall problem of animal health management, consultations with the qualified veterinaries and the results of the executed experiments introduced various approaches which should be considered for wearable animal health monitoring systems.

First of all, direct monitoring of animals vital functions makes sense in case of animals which serve for professional purposes, such as racing horses or service dogs, where the information about the animal's actual health condition can serve for the training improvements and enhancement of the animal-human interaction.

On the other hand, the wearable health monitoring system cannot supplant the deep medical check up which can detect the most serious health issues. Therefore, the users of wearable devices should not just be content with wearables' health results when the health is at stake. This can be also applied to animal welfare. The animal's health condition should always be clarified by a vet. Then, the wearable systems can serve as a complement of the animal health management.

Nevertheless, a common healthy pet, which is not aimed to be a professional at any point, does not require a continuous heart rate monitoring which is very tricky. Furthermore, the animal's handler must follow strictly instructions of the sensors/electrodes placement, etc., to obtain relevant results. Therefore, for this group of animals the undirect approach of the animal's health monitoring could be considered. It can be so, because of the matter of fact that mostly the urgent animal's health problems arise as a consequence of the animal's extreme treatment or extreme ambient environment.

### **ECG Subsystem**

The ECG heart rate monitoring subsystem adopted from [1] offers good results for remote monitoring of animals' vital functions. The designed system's performance was compared to the Holter monitor responses by the authors during several activities which is pictured in Fig.5.4. Both devices reported very similar results (only 0.34% heart beats missed by the designed system) during the resting interval and during the walking interval the responses of both systems, the designed one and the Holter monitor, slightly differed, when 5.4% of beats detected by the Holter device were missed by the designed system.

Although, the designed system is not so accurate as the Holter device, we still must keep in mind, that the designed system does not require animal fur shaving as the Holter monitor does, which makes it much more user-friendly and more appropriate for amateur daily usage of animal owners.

### **PPG Subsystem**

The PPG subsystem for heart rate monitoring based on the plethysmography principle proved that the animal hair is a significant obstacle in the wireless animal health management. The PPG system was suggested respecting the human body build and the attenuation of human tissue. Therefore, it does not take into account the animal hair at all which causes significant attenuation of the desired signal. Even though, the experiment brought sections of the measured data where the animal's heart beat was detected by the device, the results were very poor. Furthermore, the experiment was executed on a motionless animal with the PPG sensor held to the animal's body manually with

the hair removed as much as possible without shaving. When the measurement was performed over all layers of animal's hair, no desired signal was achieved.

On the other hand, if the coupling of the light (transmitted and received by the PPG device) and the animal's skin was solved, the pulse oximetry would be a great solution for non-disturbing animal heart rate monitoring. One approach to the problem of PPG sensor optical coupling with the animal's skin is also outlined in the study of [1] where the light fibers for the optical coupling improvement are suggested. Even though, the authors admitted that the designed solution is not very accurate during animal's activity and hence, the PPG system is not very reliable, it was not their biggest concern to adapt the PPG system for animal's health monitoring and they considered it more like an supplement to the ECG heart rate monitoring system. Therefore, when further improvement and experiments are executed in the field of PPG system adapting for animal usage, interesting results could be obtained.

### **Activity Tracker**

The activity tracker was designed more as an interesting supplement (or as an example of another approach to animal welfare) to the system for remote animal's vital functions monitoring. The accelerometer data were processed to achieve the step counter device, the pedometer, which could serve for animal's potential exhaustion indication or as an indicator of a disease germ when the animal's activity significantly differs from usual.

The pedometer device counted the animal steps with average fault of two missed steps per measurement. We must keep in mind that the pedometer algorithm was adapted for mid-sized dogs, which it was tested on, and even here, the results of both dogs slightly differ. In the measurements of the first dog there are more missed steps than in case of the second dog's measurement where fault steps were detected by the pedometer more often.

Nevertheless, the pedometer accuracy for a wide spectrum of animal's breeds and sizes is dependent more on the programmer's skills than on anything else and this system can be considered as reliable for the final system's design.

### **Temperature Monitor**

The fourth experiment proved the dependency of the animal's core and surface temperatures on the animal's activity. The designed system was tested only in a stable ambient environment where the temperature was at around 18°C. Nevertheless, both, the core and the surface temperatures, were rising with the animal's increasing activity and falling, or stable, during rest. Despite more measurements in various ambient temperatures and on various canine breeds should be performed to determine a convenient model for the ambient-core-surface temperatures dependencies for a correct data evaluation by a software, the surface temperature monitoring could serve quite reliably as an indicator of animal's body overheating or hypothermia.

### **SigFox Network**

Although the SigFox network is not the most suitable for the needs of wearable animal health monitoring, it offers an example of low-power data transmission over large

distances and the data visualization on the ThingSpeak cloud and on animal owner's e-mail. The experimental data transmission over SigFox network was performed for transmission of GPS coordinates because of the embedded GPS module in the Pycom device on which the SigFox network data transmission was tested.

Furthermore, the external temperature sensor was wired to the Pycom board to determine the Pycom device suitability for the designed system. Even though, the external sensors can be integrated in the system, it is not very elegant and the support from the Pycom side is not very advanced as there are not many datasheets, libraries and the firmware support of all of the hardware options is not implemented yet.

# Conclusion

This thesis is focused on the remote monitoring of animals' vital functions system design and its functionality and usability in animal remote health management assessment. The physical realization of the designed system is suggested in chapter 4 and it is clear that the hardware wiring is not challenging.

The designed system's separate subsystems were tested with respect to its functionality and reliability to the animal's health management. All designed subsystems were adapted mainly for health monitoring of dogs because they represent the most common pets and each animal species differs significantly from one to another from the body build and physiological responses point of view.

The designed subsystems for ECG heart rate monitoring and activity tracking report quite significant results and with a suitable software program for processing of the obtained data, the designed subsystems can be fully implemented into a final 'smart collar' device. On the other hand, the surface temperature and the PPG heart rate monitoring require further enhancement or measurements to report reliable results.

## Future Work

The ideas for further improvement of the designed system are described below:

- *Enhancement of PPG sensor optical coupling to the animal's skin.* The study of [1] could be continued for further improvement of the PPG heart rate monitoring in animal welfare.
- *Deeper study of temperature dependencies.* More measurements for clarifying reliable model for temperature evaluation of a wide spectrum of canine breeds/animal species in various ambient conditions should be performed.
- *Dividing the animal welfare to **professional** and **common**.* Two systems for animal welfare could be introduced as suggested in chapter 6.
- *Real-time data processing and evaluation from all sensors.* The system design was focused mainly on the system functionality, suitable components design and their hardware wiring, but the real-time data processing is the most challenging part and requires a qualified programmer and consultation of an experienced vet to evaluate the obtain data correctly.

# References

- [1] R. Brugarolas et al. “Wearable Heart Rate Sensor Systems for Wireless Canine Health Monitoring”. In: *IEEE Sensors Journal* 16.10 (May 2016), pp. 3454–3464. ISSN: 1530-437X. DOI: 10.1109/JSEN.2015.2485210.
- [2] A. Rahman et al. “Cattle behaviour classification from collar, halter, and ear tag sensors”. In: *Information Processing in Agriculture* 5.1 (2018), pp. 124–133. ISSN: 2214-3173. DOI: <https://doi.org/10.1016/j.inpa.2017.10.001>. URL: <http://www.sciencedirect.com/science/article/pii/S2214317317301099>.
- [3] MVDr. Michal Fiedler. *Vyšetření srdce*. [cit. 2019-4-26]. URL: <http://www.vetcardio.cz/cs/vysetreni-srdce>.
- [4] Judy Hermann. *Opto-Mechanical Integration of Heart-Rate Monitors in Wearable Wrist Devices*. Online. [cit. 2019-1-23]. June 2018. URL: <https://www.sensorsmag.com/components/opto-mechanical-integration-heart-rate-monitors-wearable-wrist-devices>.
- [5] Projekt sítě lékařských fakult MEFANET. *Elektrokardiografie*. Online. [cit. 2019-1-23]. Dec. 2018. URL: <https://www.wikiskripta.eu/w/Elektrokardiografie>.
- [6] Wikipedia. *Pulse Oximetry*. Online. [cit. 2019-3-1]. Feb. 2019. URL: [https://en.wikipedia.org/wiki/Pulse\\_oximetry](https://en.wikipedia.org/wiki/Pulse_oximetry).
- [7] VETgirl. *Pulse Oximetry | VetGirl Veterinary CE Blog*. Online. [cit. 2019-3-1]. URL: <https://vetgirlontherun.com/veterinary-continuing-education-pulse-oximetry-veterinary-medicine-vetgirl-blog/>.
- [8] Larry P. Tilley. *Practical use of the ECG in practice (Proceedings)*. Online. [cit. 2019-3-3]. Nov. 2010. URL: <http://veterinarycalendar.dvm360.com/practical-use-ecg-practice-proceedings>.
- [9] Wikipedia. *Holter monitor*. Online. [cit. 2019-3-2]. URL: [https://en.wikipedia.org/wiki/Holter\\_monitor](https://en.wikipedia.org/wiki/Holter_monitor).
- [10] Pet Cardiology. *Placing Holter Monitor Leads*. Online. [cit. 2019-3-2]. URL: <http://www.pet-cardiology.com/placing-holter-monitor-leads>.
- [11] @LAZHARICHIR. *Different Types of Thermometers for Dogs*. Online. [cit. 2019-3-5]. Aug. 2017. URL: <https://breedingbusiness.com/best-dog-thermometers/>.
- [12] AZoSensors. *The Working Principle and Applications of Infrared Thermometers*. Online. [cit. 2019-3-7]. June 2015. URL: <https://www.azosensors.com/Article.aspx?ArticleID=356>.
- [13] Vít Špringl. *Měření teploty - polovodičové odporové senzory teploty*. Online. [cit. 2019-1-23]. Aug. 2004. URL: <https://vyvoj.hw.cz/teorie-a-praxe/dokumentace/mereni-teploty-polovodicove-odporove-senzory-teploty.html>.
- [14] *Temperature Sensors – Types, Working and Operation*. Online. [cit. 2019-1-23]. URL: <https://www.elprocus.com/temperature-sensors-types-working-operation/>.
- [15] *DS18B20 Programmable Resolution 1-Wire Digital Thermometer*. 19-7487. Rev 5. Maxim Integrated Products, Inc. Sept. 2018.

- 
- [16] William O. Reece. *Fyziologie a funkční anatomie domácích zvířat*. 2nd ed. U Průhonu 22, Praha 7: Grada Publishing a.s., 2011.
- [17] Michal Lom and Ondřej Příbyl. *Sítě pro internet věcí v České republice*. Online. [cit. 2019-3-10]. Nov. 2017. URL: <https://elektro.tzb-info.cz/informacni-a-telekomunikacni-technologie/16519-site-pro-internet-veci-v-ceske-republice>.
- [18] Libor Michalec. *Technologie NB-IoT a LTE Cat M1 jsou krok napřed*. [cit. 2019-3-17]. Mar. 2018. URL: <https://vyvoj.hw.cz/technologie-nb-iot-a-lte-cat-m1-jsou-krok-napred.html>.
- [19] Václav Žalud. *Lecture from Radiokomunikační technologie pro IoT*. 2018.
- [20] sigfox. *Sigfox Technology Overview*. [cit. 2019-3-12]. URL: <https://www.sigfox.com/en/sigfox-iot-technology-overview>.
- [21] SIMPLECELL NETWORKS A.S. *Connecting Things*. Online. [cit. 2019-3-12]. URL: <https://simplecell.eu/>.
- [22] CRA. *Výhody CRA IoT a standardního čidla LoRaWAN*. [cit. 2019-3-16]. URL: <https://www.cra.cz/sluzby-iot>.
- [23] Vodafone. *Stvořili jsme síť pro budoucnost*. [cit. 2019-3-17]. URL: <https://www.vodafone.cz/internet-veci/>.
- [24] Mill Max Manufacturing Corp. *CONTACT SPRING LOADED SMD GOLD*. [cit. 2019-5-15]. URL: <https://www.digikey.com/product-detail/en/mill-max-manufacturing-corp/0907-3-15-20-75-14-11-0/ED5066-ND/949753>.
- [25] Analog Devices. *Analog Devices AD8232 and AD8233 Heart Rate Monitor Front End*. [cit. 2019-5-15]. URL: <https://cz.mouser.com/new/Analog-Devices/adi-ad8232-amplifier/>.
- [26] *MAX30102 High-Sensitivity Pulse Oximeter and Heart-Rate Sensor for Wearable Health*. 19-7740. Rev. 1. Maxim Integrated Products, Inc. Oct. 2018.
- [27] *MPU-6000 and MPU-6050, Register Map and Descriptions, Revision 4.2*. RM-MPU-6000A-00. Rev 34.2. InvenSense. Aug. 2013.
- [28] Jean-Luc Aufranc. *Arduino Introduces Two New IoT Boards – MKR WiFi 1010 (ESP32) and MKR NB 1500 (NB-IoT + eMTC)*. [cit. 2019-5-15]. May 2018. URL: <https://www.cnx-software.com/2018/05/14/arduino-introduces-two-new-iot-boards-mkr-wifi-1010-esp32-and-mkr-nb-1500-nb-iot-emtcc/>.
- [29] Circuit Basics. *BASICS OF THE I2C COMMUNICATION PROTOCOL*. [cit. 2019-4-26]. URL: <http://www.circuitbasics.com/basics-of-the-i2c-communication-protocol/>.
- [30] SOU technické Chotěboř. *Výpočty chlazení elektronických součástí s řešenými příklady*. [cit. 2019-5-21]. URL: <http://www.souch.cz/dok/e/chlazení.pdf>.
-